RWTH

PITHA 94/54

März 1995

Beam Position Measurements by Modulation of Quadrupole Strengths

Ina Reichel

III. Physikalisches Institut, Technische Hochschule Aachen
52056 Aachen, Germany

PHYSIKALISCHE INSTITUTE
RWTH AACHEN
52056 AACHEN, GERMANY

Beam Position Measurement
by Modulation
of Quadrupole Strengths

von

Ina Reichel

Diplomarbeit in Physik

vorgelegt der

Mathematisch-Naturwissenschaftlichen Fakultät der

Rheinisch-Westfälischen Technischen Hochschule Aachen

im

März 1995

angefertigt im

III. Physikalischen Institut A

bei

Priv. Dozent Dr. M. Tonutti

Abstract

In this diploma thesis a new method to measure the beam position with respect to the center of the quadrupole magnets is described. This technique, based on the modulation of the quadrupole strength and therefore called k-modulation, is used at LEP to calibrate the orbit monitors.

The method of k-modulation is explained. The hardware that is used to do the measurements is described. It is explained how the offsets of the orbit monitors are calibrated. The results of the calibration of the orbit monitor system are given and effects on the performance of LEP are discussed.

Contents

Introduction

With e^+e^--colliders such as LEP[1] at CERN[2] close to Geneva, Switzerland, the constituents of matter are investigated [LEP84]. Its main objective is the study of the electro-weak interaction. During the last years it was operated at an energy of about 46 GeV per beam to measure the properties of the Z boson which was discovered at the CERN $p\bar{p}$-collider SPS[3] in 1983.

Using the results from millions of decays of Z bosons different parameters of the Standard Model can be tested to high accuracy. The mass of the Z boson is now determined with a relative precision of $7.7 \cdot 10^{-5}$ [Par94]. The existence of a fourth light neutrino could be excluded after studies of the width of the resonance curve of the Z.

LEP is a storage ring where four physics experiments are located at the collision points. Electron and positron beams are circulating for many hours in the vacuum chamber. Dipole magnets are used to bend the trajectories of the particles in order to keep them on circular paths. Quadrupole magnets act as lenses to keep the beams from diverging.

For the optimum performance of LEP the beams are kept as close as possible to the centers of the quadrupole magnets. Beam orbit monitors installed close to the quadrupoles measure the beam position and an orbit correction system minimizes the RMS of the beam position at the monitors. However, the accuracy of the orbit monitors is limited: If the beam travels through the center of a quadrupole, the reading from the nearby monitor is not necessarily zero. This difference is referred to as offset. Possible sources of the offset are a mechanical misalignment of the orbit monitors with respect to the magnets or the electronics for the signal treatment.

In this thesis a method is described to measure the monitor offsets : The strength of a quadrupole is modulated at a well defined frequency. If the beam travels off center through the quadrupole it oscillates at this frequency. The amplitude of the oscillation is proportional to the displacement of the beam. The beam position monitor reading for vanishing oscillation amplitude yields the monitor offset. This method to determine the monitor offsets does not perturb the normal operation and therefore does not require dedicated beam time.

A different method to measure the offsets of the beam orbit monitors has been used elsewhere [CESR83, SLC91, MAX94, HERA94]: The orbit is measured with all quadrupoles at nominal strength. Then the strength of one quadrupole is changed. If the beam is not centered in this quadrupole the orbit changes. This procedure is repeated with different beam positions in the quadrupole until the orbit does not change by changing the quadrupole strength. This technique can not be used during luminosity operation because it requires dedicated beam time. At CESR the accuracy of the measurement was improved by averaging over several cycles of changing the quadrupole strength [CESR85].

In the first chapter different concepts of focusing ('weak' and 'strong') are described and the

[1] Large Electron–Positron Collider

[2] Conseil Européen pour la Recherche Nucléaire

[3] Super-Proton-Synchrotron

influence of quadrupole strength modulation on the beam dynamics is discussed.

Then the method to calibrate the beam orbit monitors and the hardware to perform the measurements are described. How to extract from the measurements the offsets of the beam position monitor is discussed in the following, and the results for all monitors calibrated during 1994 are presented. Finally the influence of the position monitor calibration on the LEP performance is discussed.

Chapter 1

Quadrupoles in Storage Rings

1.1 The Principle of Storage Rings

In storage rings magnetic fields are used to guide the particles. Hence one can derive the equation of motion from the equation describing the Lorentz force. For particles traveling in a magnetic field the equation of motion is (m is the relativistic mass of the particle; in LEP electrons and positrons are highly relativistic):

$$\frac{d\vec{v}}{dt} = \dot{\vec{v}} = \frac{q}{m}\,\vec{v} \times \vec{B} \tag{1.1}$$

Consider a storage ring where the magnetic bending field is constant and the particles are assumed to be moving only in the plane perpendicular to the magnetic field. Since the field is constant as a function of the particle position the particles will move on a circle with the radius $\rho = \frac{mv}{eB}$. At this radius the centrifugal force compensates the Lorentz force. The revolution frequency of this motion is the so-called cyclotron-frequency

$$\omega = \frac{eB}{m} \tag{1.2}$$

All particles that start at the same place with the same velocity $\vec{v}$, perpendicular to the magnetic field, will travel on the same trajectory. Unfortunately not all particles have identical initial conditions and their trajectories will be different after a short time. Consider a particle with a small velocity component in the direction of the magnetic field: If no other force than the force from the deflecting magnets acts on the particle, the distance to the particles with no velocity component in that direction will increase until the particle finally hits the wall of the vacuum chamber. This shows that one needs restoring forces to obtain stable beams of circulating particles.

Before considering these forces in detail, let us introduce the coordinate system for circular accelerators and storage rings (see also Fig. 1.1): Usually one assumes the ideal particles to move only in the horizontal plane. The coordinate system moves along the ring on the way of an ideal particle (which moves on a circle with the radius ρ). The coordinate along the ring is s. Deviations from this ideal trajectory in the horizontal plane are described by the coordinate x and in the vertical plane by y which are both perpendicular to s.

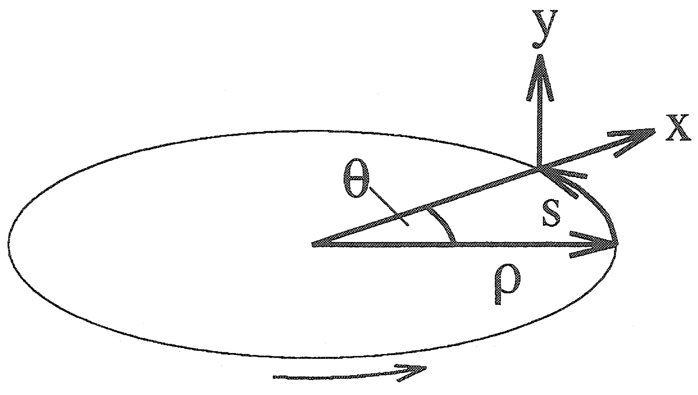

Figure 1.1: Coordinate system in a storage ring which follows a particle on the ideal orbit.

1.2 Weak Focusing

Consider now a motion in the horizontal plane, i.e. $y \equiv 0$: If a particle travels at a radius $r < \rho$ one wants the Lorentz force to be smaller than the centrifugal force to bring the particle back to the ideal orbit, and vice-versa if $r > \rho$. This leads to a set of equations [JRPS92]:

$$evB_y(r) \begin{cases} < \frac{mv^2}{r} & \text{for} \quad r < \rho \\ > \frac{mv^2}{r} & \text{for} \quad r > \rho \end{cases} \tag{1.3}$$

Consider a particle with a small deviation from the ideal orbit:

$$r = \rho + x = \rho\left(1 + \frac{x}{\rho}\right) \tag{1.4}$$

$$\frac{mv^2}{r} \approx \frac{mv^2}{\rho}\left(1 - \frac{x}{\rho}\right) \tag{1.5}$$

$$evB_y(r) \approx evB_0\left(1 - n\,\frac{x}{\rho}\right) \quad \text{with} \quad B_0 = B_y(\rho) \tag{1.6}$$

n in Eq. 1.6 is the so-called field index. It describes the gradient of the magnetic field at the ideal radius ρ:

$$n = -\frac{\rho}{B_0}\left(\frac{\partial B_y}{\partial r}\right)_{r=\rho} \tag{1.7}$$

Using Equations 1.3, 1.4 and 1.6 one obtains the condition $n < 1$ if one wants to keep a particle close to the ideal orbit in the horizontal plane.

Consider now $n \equiv 0$ which corresponds to the case of a homogeneous magnetic field. To keep the particles close to the ideal orbit in the horizontal plane the condition given in Eq. 1.3 has to be fulfilled. With $n \equiv 0$, B_y does no longer depend on r, and therefore Eq. 1.3 is still valid. The particles will move on different circles but with the same radius. This means that particles starting from the same point with the same energy will meet again every turn at the same point of the ring (Fig. 1.2). This way of focusing the beams is called geometrical focusing. In accelerators with weak focusing the largest part of the focusing in the horizontal plane ($y \equiv 0$) comes from geometrical focusing. However geometrical focusing alone is insufficient to obtain a stable particle beam as already shown for a particle with a velocity component in the direction of y.

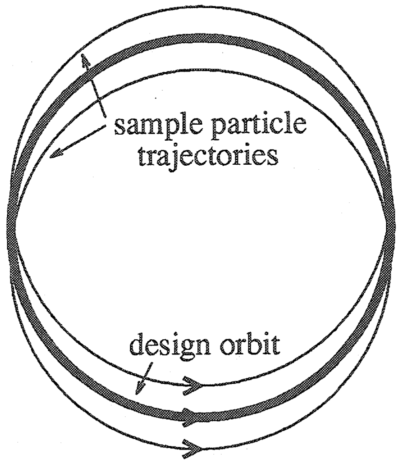

Figure 1.2: Geometrical focusing: The particles start at the same point but with different angles and have no velocity component perpendicular to the shown plane. The magnetic field is supposed to be homogeneous. The particles will meet at the same point after each revolution. All trajectories have the same radius if all particles have the same momentum.

To keep these particles close to the ideal orbit one needs a (linear) restoring force in the vertical plane $F_y = -C \cdot y$ ($C = const.$), which is exerted by a horizontal component of the magnetic field $B_x = -C' \cdot y$. From $\nabla \times \vec{B} = 0$ (Maxwell equations) one obtains:

$$\frac{\partial B_x}{\partial y} = \frac{\partial B_y}{\partial x} \equiv \frac{\partial B_y}{\partial r} \tag{1.8}$$

r is the distance of the particle to the center of the ring ($r = x + \rho$). From Eq. 1.8 follows that a varying horizontal component of the magnetic field requires a change of the vertical component of the field in the horizontal direction. Hence B_y has to decrease if r increases (see Fig. 1.3). If $\frac{\partial B_y}{\partial r}$ is negative, the field index is positive ($n > 0$; Eq. 1.7).

Two conditions for the field index have to be fulfilled to achieve stability in the horizontal and in the vertical plane. For the horizontal plane the condition was $n < 1$. Together with $n > 0$ for the vertical plane one gets $0 < n < 1$.

For small amplitudes in x and y the restoring forces are linear. This leads to harmonic oscillations around the ideal orbit. The differential equations for these oscillations are:

$$\ddot{x} + (1 - n)\,\omega_0^2\, x = 0 \tag{1.9}$$

for the horizontal motion and

$$\ddot{y} + n\,\omega_0^2\, y = 0 \tag{1.10}$$

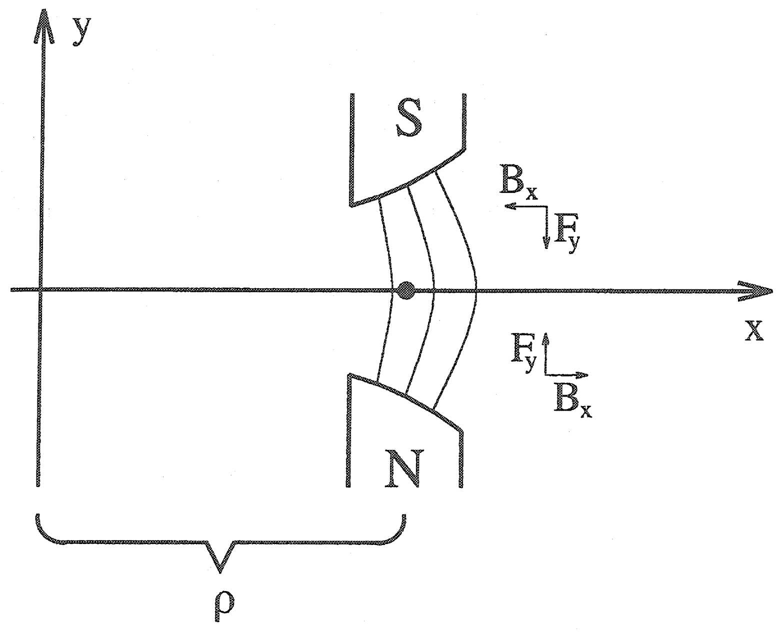

Figure 1.3: The shape of the magnetic field around the ideal orbit for weak focusing: One needs a varying horizontal component of the magnetic field to achieve stability in the vertical plane. ρ is the radius of the ideal orbit. x is the deviation from the ideal orbit in the horizontal plane.

for the vertical motion ($\omega_0 = \frac{eB_0}{m}$). The revolution frequency of the particles is $f_0 = \frac{\omega_0}{2\pi}$. From Equations 1.9 and 1.10 one obtains for the frequencies of the so-called betatron oscillations:

$$f_x = \sqrt{1-n}\, f_0 \qquad \text{and} \qquad f_y = \sqrt{n}\, f_0 \tag{1.11}$$

For an accelerator with weak focusing ($0 < n < 1$) the frequency of these oscillations is lower than the revolution frequency, i.e. there is less than one oscillation per turn. This leads to the great disadvantage of the weak focusing: For accelerators with a large circumference the deviations of the particle trajectories from the ideal orbit become very large, which requires large aperture vacuum chambers and magnets. To reduce the wavelength and therefore increase the frequency of the betatron-oscillations a focusing system with $|n| \gg 1$ is required, which is in contradiction to the condition $0 < n < 1$ for a guiding field independent of the azimuthal angle. The solution is to build accelerators with separately bending and focusing magnets where the field increases ($n \ll -1$) or decreases ($n \gg 1$) strongly with the radius (strong focusing).

1.3 Strong Focusing

Strong focusing is based on the use of alternating focusing and defocusing lenses. From light optics one obtains an equation to describe the focal length f_{tot} of a structure of two lenses with the focal lengths f_1 and f_2 separated by a distance d (thin lens approximation):

$$\frac{1}{f_{tot}} = \frac{1}{f_1} + \frac{1}{f_2} - \frac{d}{f_1 f_2} \tag{1.12}$$

Consider now a focusing and a defocusing lens with the same strength, i.e. $f_1 = -f_2 = f$. In this case the total focal length is $f_{tot} = \frac{d}{f^2} > 0$ which means that the structure is focusing. In accelerators a structure like that is called FODO. It is shown in Fig. 1.4. In the FODO-structure of accelerators and storage rings, quadrupole magnets play the role of the lenses. How they work will be described later in chapter 1.7.

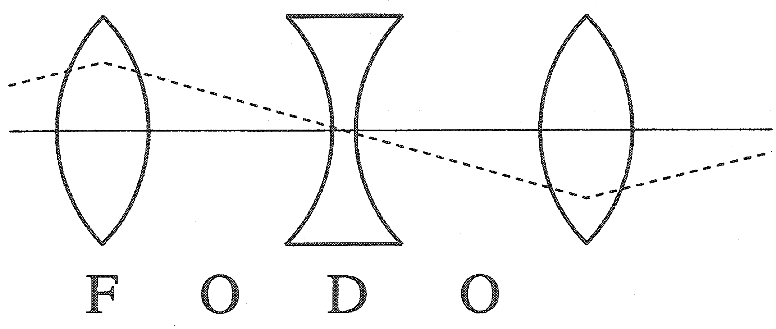

Figure 1.4: The principle of the FODO cell. F and D denote focusing and defocusing. Each cell consisting of a focusing and a defocusing lens is focusing.

1.4 Betatron Oscillations

We will now look at the equations of motion for a particle moving through the ring. For all calculations only linear beam dynamics[1] will be used. The equation of motion in the horizontal plane is [Wil92]:

$$x'' - \left(k - \frac{1}{\rho^2}\right) x = \frac{1}{\rho} \frac{\Delta p}{p_0} \tag{1.13}$$

where k is the focusing strength (the exact definition of k will be given later in Eq. 1.26) and ρ the bending radius. p_0 is the nominal momentum and Δp the momentum deviation of the considered particle with respect to the nominal one. All parameters except $\frac{\Delta p}{p_0}$ depend on s and are periodic functions because the magnetic fields are assumed to be constant with time. In the case of weak focusing k is independent of s.

In the vertical plane the situation is simpler, because it is assumed that there are no bending forces:

$$y'' + k\,y = 0 \tag{1.14}$$

In the following calculations all particles are considered to have the same momentum ($\Delta p = 0$) which makes the right side of Eq. 1.13 equal to zero.

In a machine with strong focusing like LEP ($|k| > 0.01\,\frac{1}{m^2}$ and $\rho \approx 3$ km) $\frac{1}{\rho^2} \ll |k|$ is valid, which implies that the equations of motion are the same for both planes. It is therefore sufficient to study the problem for one plane.

[1] Only fields which are constant or vary linearly with the displacement are considered. The fields are assumed to be constant with time.

For each plane we have a set of two equations:

$$y''(s) + k(s)\, y(s) = 0 \tag{1.15}$$

$$k(s+L) = k(s) \tag{1.16}$$

where L is the length of the ring. Equation 1.16 shows that k is periodic with the length of the ring. Equation 1.15 is called Hill's equation. It is similar to the equation of a harmonic oscillator with the difference that the restoring force is space-dependent. $y(s)$ is therefore an oscillation around the ideal orbit. This oscillation is the so-called betatron oscillation. The differential equation can be solved to yield:

$$y(s) = A\, u(s)\ \cos(\psi(s) + \phi) \tag{1.17}$$

ϕ determines the phase of the oscillation and A the amplitude. Both depend only on the starting conditions. $u(s)$ and $\psi(s)$ are independent of the starting conditions and depend only on the magnetic fields. Equation 1.17 together with Eq. 1.15 leads to a new differential equation:

$$u''(s) - \frac{1}{u^3(s)} - k(s)\, u(s) = 0 \tag{1.18}$$

This equation has no analytical solution but it can be solved numerically even for large rings like LEP with hundreds of magnets. For convenience the β-function $\beta(s) := u^2(s)$ and the emittance ε ($\sqrt{\varepsilon} := A$) are introduced. They will be discussed in detail later. We obtain the following equation for $y(s)$:

$$y(s) = \sqrt{\varepsilon}\,\sqrt{\beta(s)}\ \cos\left(\psi(s) + \phi\right) \tag{1.19}$$

where

$$\psi(s) = \int_0^s \frac{d\sigma}{\beta(\sigma)} \tag{1.20}$$

From Eq. 1.20 follows that $\psi(0) = 0$. The total number of oscillations per revolution is given by:

$$Q = \frac{1}{2\pi}\,\psi(L) = \frac{1}{2\pi}\int_0^L \frac{d\sigma}{\beta(\sigma)} \tag{1.21}$$

Q is called the betatron-tune. The theoretical values for LEP for the presently used beam optics are $Q_x = 90.287$ and $Q_y = 76.189$. The amplitude of the betatron oscillation is given by the envelope $E(s) = \sqrt{\varepsilon\beta(s)}$. The phase of the oscillation is given by $\psi(s) + \phi$. Figure 1.5 shows the meaning of the envelope. It defines the beam-size at the point s.

$\sqrt{\beta}$ indicates the size of the beam at a certain place. In a FODO-structure it is large at the focusing lens and small at the defocusing lens. At the collision points one wants β to be as small as possible to increase the particle density and enhance the collision rate. The emittance ε represents the area of the beam in the phase space. As long as there are only conservative forces, it is constant (Liouville's theorem). β and ε can be conveniently used to calculate the RMS-beam size, assuming a Gaussian particle distribution: $\sigma = \sqrt{\beta\varepsilon}$.

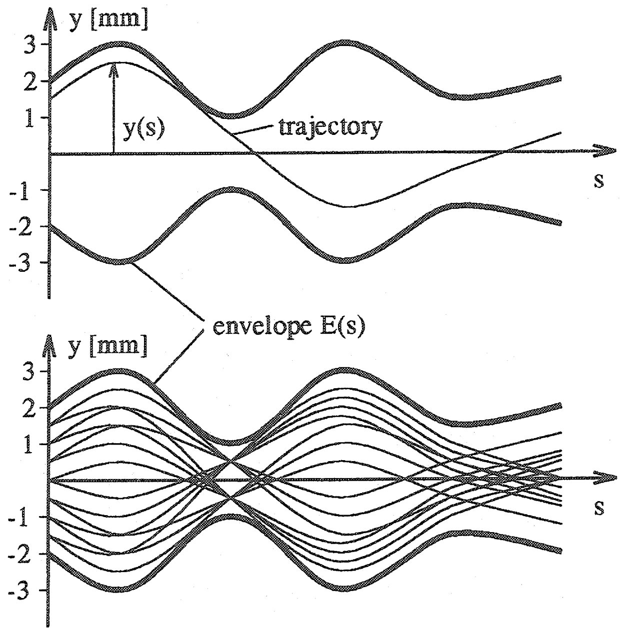

Figure 1.5: Different trajectories $y(s)$ within the envelope $E(s)$ of the beam. The top part shows a single trajectory. The bottom part shows some different ones. As there are many particles in the beam which all have different trajectories the envelope $E(s)$ defines the beam-size.

Another parameter widely used is the α-function which is proportional to the slope of the β-function:

$$\alpha(s) := -\frac{\beta'(s)}{2} \tag{1.22}$$

The parameters α, β and ψ are the Twiss-parameters. Sometimes one also uses $\mu = \frac{\psi}{2\pi}$.

1.5 Transfer Matrix for Beam Optics

The position of a particle beam can be calculated at any point in the ring, if the position and the angle at the starting point are known as well as all (magneto-)optical elements between the two points. Like for light optics a transfer matrix can be used to calculate the trajectory of a particle with a given position x_0 and angle x_0' (at the starting point) through the optical elements of the ring:

$$\begin{pmatrix} x(s) \\ x'(s) \end{pmatrix} = \mathcal{M}(s) \begin{pmatrix} x_0 \\ x_0' \end{pmatrix} \tag{1.23}$$

Matrix $\mathcal{M}(s)$ can be calculated with Eq. 1.19 as shown in [Wil92]. The matrix depends only on the α- and β-functions and the phase ψ of the betatron oscillations:

$$\mathcal{M}(s) = \begin{pmatrix} \sqrt{\frac{\beta_s}{\beta_0}}\,(\cos\psi_s + \alpha_0 \sin\psi_s) & \sqrt{\beta_s\beta_0}\,\sin\psi_s \\ \frac{(\alpha_0-\alpha_s)\cos\psi_s - (1+\alpha_0\alpha_s)\sin\psi_s}{\sqrt{\beta_s\beta_0}} & \sqrt{\frac{\beta_0}{\beta_s}}\,(\cos\psi_s - \alpha_s \sin\psi_s) \end{pmatrix} \tag{1.24}$$

with $\beta(0) = \beta_0$, $\alpha(0) = \alpha_0$ and $\psi(0) = 0$. α_s, β_s and ψ_s are the values of these functions at the place s. This matrix is valid for an accelerator without coupling between the horizontal and vertical plane.

1.6 Misalignments and Closed Orbit

If all focusing elements are exactly aligned, a particle, which starts with no displacement and no angle with respect to the ideal orbit (and nominal energy), will continue to travel through the centers of all elements on a closed curve, the ideal closed orbit. Until now we have considered only this ideal case.

For all calculations we have assumed a structure without any imperfections like misalignments or field errors. However for a real structure this no longer holds. E.g. in an real structure the lenses are not perfectly aligned. The effect of a slightly misaligned lens is shown in Fig. 1.6. Due to the misalignment of a lens a deflecting force acts onto the particle. The oscillation that is induced there continues around the whole ring and the particle will not travel through the centers of the following lenses anymore.

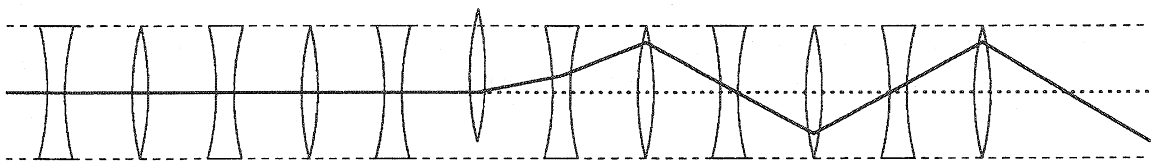

Figure 1.6: Effect of a misaligned lens on a trajectory in a FODO-structure.

This shows that for a non-ideal structure the ideal orbit does not exist anymore. But there still exists a closed curve that describes the orbit of a particle with nominal momentum through the structure [Wie93]. This new equilibrium orbit no longer passes through the centers of all magnets. It is called the closed orbit. It is shown in Fig. 1.7.

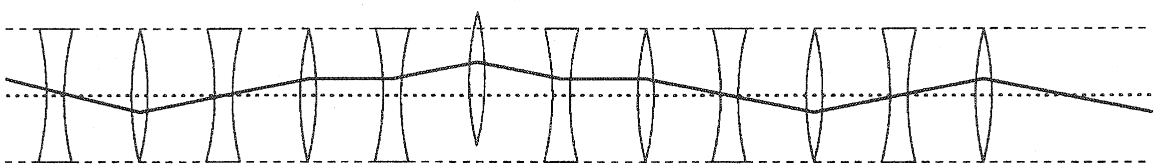

Figure 1.7: Effect of a misaligned lens on the closed orbit in a FODO-structure. In this figure and in Fig. 1.6 it is not assumed that all lenses have the same focal length, i.e. strength, as the plot is only schematic.

The performance of LEP depends critically on the closed orbit which is therefore optimized in the following way: The orbit is measured with 504 beam orbit monitors attached to quadrupoles (as there are about 800 quadrupoles in LEP, not every quadrupole is equipped with a beam orbit monitor).The orbit correction is performed with dipole correction magnets. The goal of the orbit correction is to minimize the orbit deviations in the quadrupoles. However, due to misalignments between the quadrupoles and the monitors as well as due to the electronics the accuracy is limited:

The monitor does not give zero beam position when the beam travels through the center of the quadrupole. The orbit monitor reading corresponding to the center of the quadrupole is referred to as offset.

The most important parameter describing the performance of a collider is the luminosity, because the number of interactions between the electrons and positrons is proportional to the luminosity:

$$\mathcal{L} = \frac{N_{e^+} N_{e^-} f_{rev} b}{4\pi \sigma_x \sigma_y} \tag{1.25}$$

b is the number of bunches per particle type (the particles in a storage ring are not distributed evenly around the ring but come in packets called bunches; in 1994 LEP was operated with four or eight bunches per particle type); N_{e^+} and N_{e^-} are the numbers of positrons and electrons per bunch, respectively; f_{rev} is the revolution frequency; σ_x and σ_y are the beam-sizes in the corresponding planes at the collision point.

The (unknown) offsets of the orbit monitors can affect the luminosity. As a consequence, in LEP, one usually does not correct the orbit to be as flat as possible, but towards a reference which has given the highest luminosity. This reference is called the 'Golden Orbit' and is found during luminosity runs by trial and error. In the '94 run of LEP it took about one month to find the 'Golden Orbit'. What makes this orbit 'golden' is not yet understood and therefore still studied [Col94, HSch94].

1.7 The Quadrupole Strength k

Quadrupoles are the lenses that are used for the strong focusing. In contrary to optical lenses they are focusing in one plane and defocusing in the other. The FODO-structure consists of quadrupoles, where every second one of them is rotated by 90 degrees along its axis with respect to the others in order to get a focusing and a defocusing lens in each plane with two quadrupoles.

The parameter describing the strength of a quadrupole is the normalized gradient of its field and is called k. It is defined as

$$k = \frac{e}{p} \frac{dB_y}{dx} \tag{1.26}$$

The sign is defined such that for $k < 0$ the quadrupole is focusing in the horizontal plane and for $k > 0$ it is defocusing. It is the same k already introduced in Eq. 1.13. In LEP the strongest quadrupoles are the superconducting quadrupoles at both sides of the four LEP-experiments. They have $|k| \approx 0.16 \frac{1}{m^2}$. All other quadrupoles in LEP have a strength that is about one order of magnitude smaller.

The focal length of a quadrupole is obtained from k and the length l of the quadrupole:

$$\frac{1}{f} = k \cdot l \tag{1.27}$$

The focal length of the 2 m long superconducting quadrupoles is about 3 m, which corresponds to their distance to the interaction point.

Figure 1.8 shows the cross section of a quadrupole magnet. In the center of the quadrupole the field vanishes. Within the vacuum chamber the strength of the field rises linearly with the distance to the center, which means that the force on a particle is proportional to its displacement. The direction of the force depends on the sign of the charge of a particle and its direction

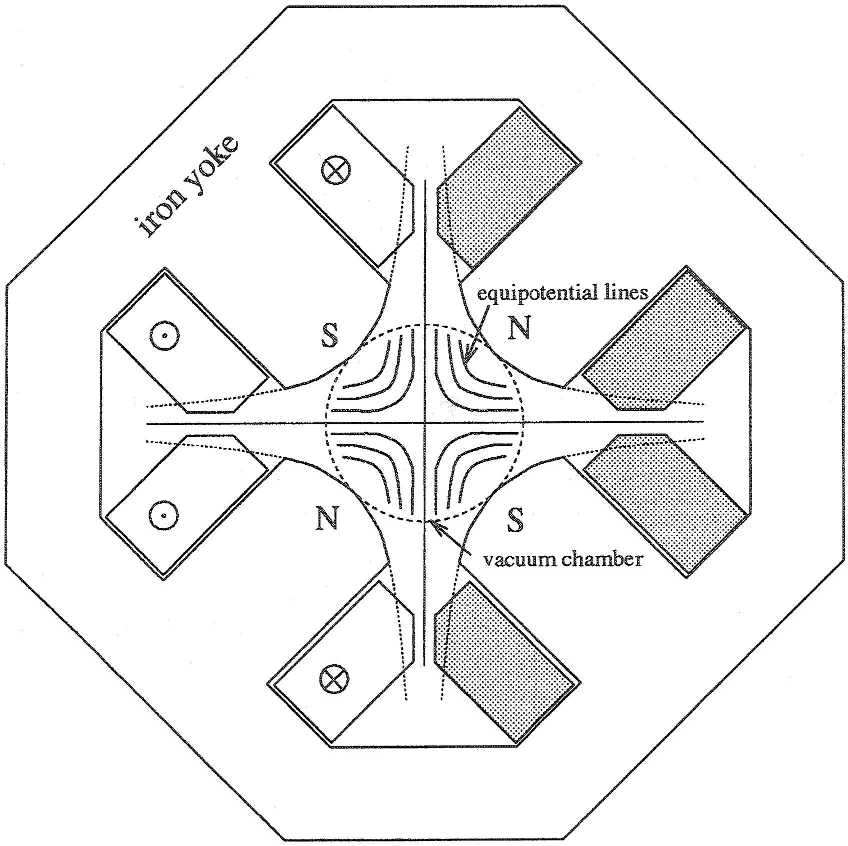

Figure 1.8: Cross-section of a quadrupole magnet and the lines of equal potential of the magnetic field produced by it. In LEP the diameter of the vacuum chamber is of the order of magnitude of 10 cm (it is not constant around the ring; in the arcs it is elliptic).

of motion. If one considers a particle moving through the quadrupole in one direction and its anti-particle moving in the opposite direction one plane will be focusing for both and the other defocusing for both.

1.8 Modulation of the Quadrupole Strength

We consider now a vertically focusing quadrupole. A modulation of the strength of the quadrupole changes the focusing strength. The effect of two different quadrupole strengths is shown in Fig. 1.9.

Assume that the quadrupole is located at a position s_1 in the ring: If the quadrupole strength k is changed by a value Δk ($\frac{\Delta k}{k} \approx 10^{-4}$ in our experiments) the deflection of the particle changes by a value $\Delta y'(s_1)$ (in rad)

$$\Delta y'(s_1) = \Delta k \cdot l \cdot \Delta y(s_1) \tag{1.28}$$

$\Delta y(s_1)$ is the displacement of the beam in the quadrupole and l the length of the magnet. The additional deflection changes the closed orbit. The additional displacement at a point s_2 anywhere

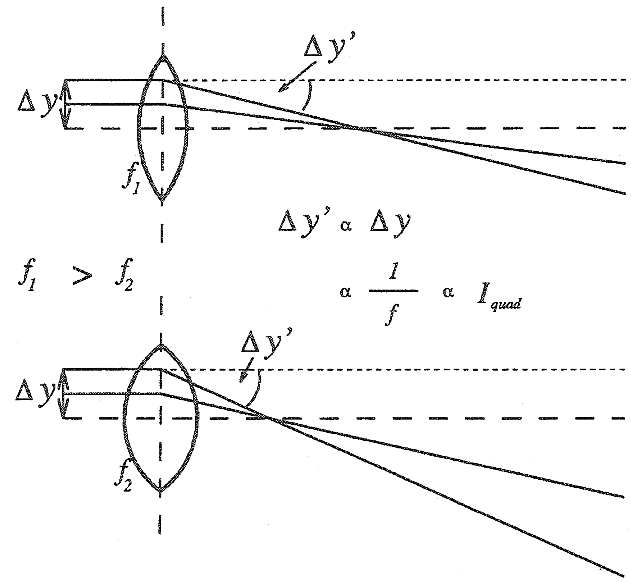

Figure 1.9: Effect of two different quadrupole strengths on a particle passing the quadrupole with a certain displacement Δy. The strength of the kick $\Delta y'$ depends on the quadrupole strength which is proportional to the current in the windings of the magnet. The kick is also proportional to Δy.

in the ring – due to this additional deflection – can be calculated with the following formula [RSch93], assuming $\psi(s_2) > \psi(s_1)$:

$$\Delta y(s_2) = \frac{\sqrt{\beta(s_1)\,\beta(s_2)}\;\cos(\psi(s_1) - \psi(s_2) - \pi Q_y)}{2\,|\sin(\pi Q_y)|}\;\Delta y'(s_1) \qquad (1.29)$$

Q_y is the vertical betatron-tune according to Eq. 1.21. The displacement in the horizontal plane can be obtained in a similar way. From Eq. 1.29 it becomes clear that a change of the deflection in a magnet can be measured as a displacement (almost) everywhere around the ring. If one modulates the strength of one quadrupole with a certain frequency (and if this frequency is much lower than the revolution frequency) and the beam goes through that quadrupole off center, the beam starts oscillating at this frequency. The amplitude of this oscillation is proportional to Δk and to the displacement of the beam in the quadrupole where the strength is modulated. In our measurements the amplitude of the oscillation around the ring was of the order 1 μm, which is much smaller than the beam size.

The measurements were made with the quadrupole strengths modulated at frequencies between 0.8 Hz and 2.0 Hz for most of the quadrupoles and between 10.0 Hz and 15.6 Hz for the quadrupoles close to the interaction points. This frequencies do not disturb the performance of LEP because they are very low compared to the revolution frequency which is 11246 Hz. Also the small amplitude already mentioned is smaller than other beam oscillations which can not be avoided. For LEP this method has the advantage that the calibration of the orbit monitors does not require dedicated beam time but can be applied during normal operation.

As the amplitude of the beam oscillation is proportional to the displacement in the quadrupole this is a convenient way to measure the beam position in the quadrupole. In particular, the amplitude of the beam oscillation can be minimized by centering the beam in the quadrupole. If at the same time the position is measured with the adjacent monitor, the offset of the monitor with respect to the center of the quadrupole is known.

In this paper I sometimes use the expression 'modulated quadrupole(s)'. With this term I refer to the quadrupole(s) where the strength of the magnetic field is modulated by changing the current in the windings.

1.9 Influence on Machine Parameters

As we want to measure continuously during the normal operation of LEP when the four LEP-experiments take data, any interference between our measurements and the operation has to be avoided. Parameters, which might be affected by the modulation of the quadrupole strength, are the betatron tunes, the closed orbit, the luminosity and the particle background in the four LEP-experiments. I will give estimates on the influence here. In chapter 5.3 I will give a short description of the observed influences.

The change of the betatron tune due to the change of the quadrupole strength is estimated [Wie93]:

$$\Delta Q \approx -\frac{\beta_{quad}}{4\pi}\int \Delta k \, ds \tag{1.30}$$

The largest contribution to the tune change comes from the k-modulation of the superconducting quadrupoles, because there Δk and also β_{quad} are larger than at all other places in the ring. With $\beta_{quad} = 383$ m, $\frac{\Delta k}{k} \approx 10^{-4}$ and $k \approx 0.16\frac{1}{m^2}$ one obtains $\Delta k \approx 1.6 \cdot 10^{-5}\,\frac{1}{m^2}$. With a length of 2 m this gives a tune change of the order of $\delta Q = 0.001$ (compare with $Q_y \approx 76.2$). Such a small tune change has no influence on the performance of LEP, in particular it does not change the luminosity.

Another important observable is the background of particles in the four LEP-experiments. The background is induced by high energy electrons and positrons which are lost out of the beam and by synchrotron radiation from the particles traveling through magnetic fields. The background depends critically on the vertical closed orbit, but changing the closed orbit in the range of micrometers with low frequencies should not affect the experiment's backgrounds.

Chapter 2

Experimental Setup

2.1 k-modulation at LEP

The beam transport system of LEP (Fig. 2.1) consists of eight arcs and eight straight sections. The total length is 26.66 km which makes it the largest existing accelerator. In the middle of each straight section is an interaction point (IP) where the particles can collide. The interaction points are numbered clockwise (the direction of the positrons) from 1 to 8. The four LEP-experiments (L3, ALEPH, OPAL and DELPHI) are located at the even interaction points.

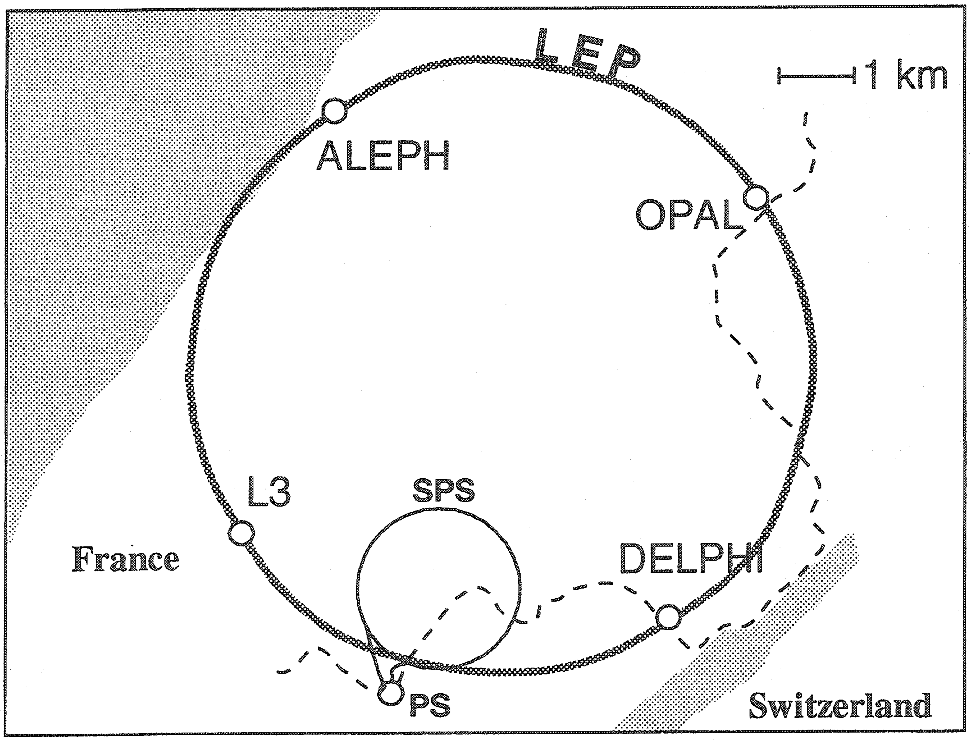

Figure 2.1: Schematic map of LEP. The PS and the SPS are smaller accelerators that are used to accelerate the electrons and positrons prior to their injection into LEP. L3, ALEPH, OPAL and DELPHI are the four LEP-experiments which are located at the even numbered interaction points. The positrons move clockwise, the electrons counterclockwise. The figure is taken from [L3Col].

2.2 The Quadrupoles

The beam transport system in LEP is symmetric around each interaction point. In four of the straight sections the beams are colliding in the detectors of the LEP-experiments. To maximize the luminosity the beams are strongly focused to the interaction (i.e. collision) points in the so-called low-β-insertions. In the arcs the β-function is between 30 and 120 m, whereas at the interaction points $\beta_x = 2$ m and $\beta_y = 0.05$ m. In the vertical plane the β-function has its largest values (almost 400 m) in the superconducting quadrupoles which are about 5 m away from the interaction points.

The 'naming' of the quadrupoles is the following: All even straight section quadrupoles are named according to the following convention: QSi.Rj or QSi.Lj where j is the number of the straight section (2,4,6 or 8) and i is the number of the quadrupole (0 to 12). The numbering starts from the interaction point. The superconducting quadrupole closest to the experiment has number 0. R or L denote the side of the interaction point when looking from the center of the LEP ring. In the straight sections almost all quadrupoles with even numbers are focusing in the vertical plane, these with odd numbers are focusing in the horizontal plane. The QS0s are the only superconducting quadrupoles in LEP.

Beam orbit monitors are attached to almost all quadrupoles in the straight sections. They are fixed to the yokes of the quadrupoles at one side of the magnet.

During most of the time of the '94 run only the strength of the quadrupoles in the straight section around interaction point 8 could be modulated as well as the strength of the QS0s and QS1s at all even interaction points. Only during the last three weeks of the '94 run we could modulate the strength of the quadrupoles in the other even numbered straight sections. Until now it is not possible to modulate the strength of any arc quadrupoles. This is foreseen – at least for one arc – for the running period in 1995 run.

The modulation is done in two different ways:

- The strengths of the QS0s and QS1s are modulated by changing the current in the windings of the magnet. For technical reasons the modulation of the reference current is not sine-like, but a rectangular function. Due to the inductance of the magnet and the vacuum chamber the magnetic field does not change as fast as the reference current. Therefore the changes of the magnetic field are smooth. In addition the higher harmonics of the frequency are in the range above 30 Hz (the lowest frequency used for these quadrupoles is 10 Hz) where we do not modulate any quadrupoles and therefore it does not disturb the results. The frequencies used for these quadrupoles are in the range between 10 Hz and 15.6 Hz. During most of the time in 1994 frequency changes of up to 0.05 Hz from the required value were present. Now the control of the modulation is done in a different way which is leading to a stable frequency.

- For symmetry reasons the other magnets in the straight section are powered in pairs, with only one power converter for each pair of magnets (e.g. QS4.L8 and QS4.R8 are powered by the same power converter). With a modulation of both quadrupoles together it is impossible to determine which part of the orbit oscillation is produced by each of them. Therefore those quadrupoles are equipped with additional windings (back-leg windings) that are powered by separate power converters. These power converters can each modulate one quadrupole at a time with a sine-function. All quadrupole magnets in the even straight sections (except the QS0s and QS1s) are already equipped with back-leg windings, but most of the time in the 1994 running period we had only two power converters for the additional windings at interaction point 8. The modulation by back-leg windings has one drawback: If the strength of one quadrupole is modulated, the change in the magnetic field induces a voltage in the main windings of this quadrupole and therefore changes the current in the windings. This current also flows to the other quadrupole which is connected to the same power converter. Therefore the strength of the second quadrupole changes as well. To avoid this effect we choose frequencies below 2 Hz for these quadrupoles because for such low frequencies the current change is negligible.

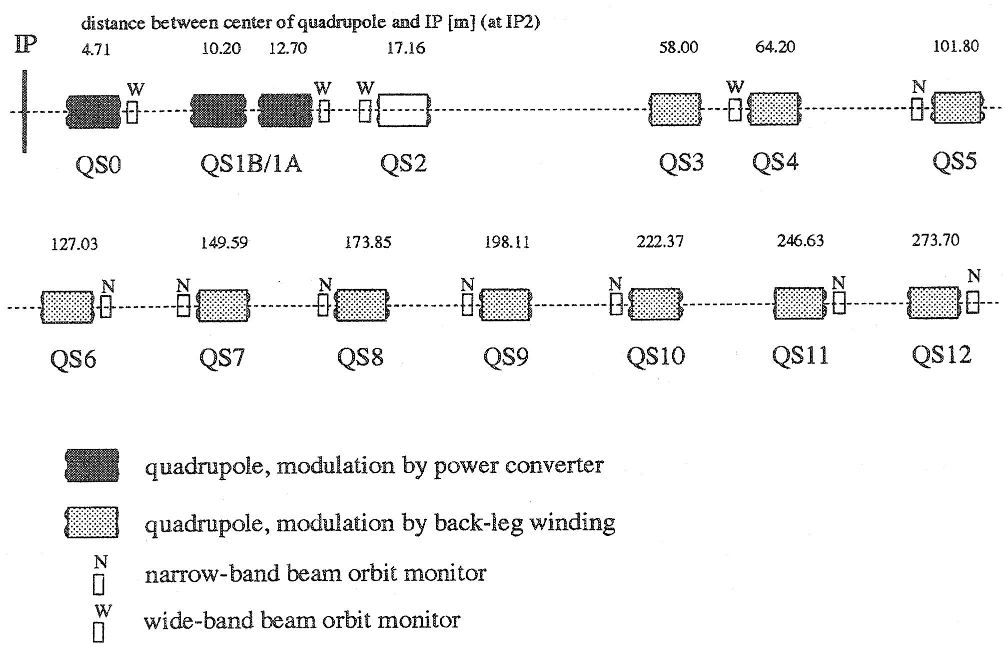

Figure 2.2: The straight section on the right side of interaction point 2. QS1 consists of two separate quadrupoles powered by one power converter. QS0 is superconducting, all other magnets are normal conducting. Only the quadrupoles and the beam orbit monitors drawn. All straight sections are more or less identical and are symmetric with respect to the interaction point. Sizes and distances are not to scale.

Figure 2.2 shows half of the straight section around interaction point 2. It shows how the quadrupole strengths are modulated and on which side of the quadrupoles the beam position monitors are located.

The strength of the modulation is of the order of $\frac{\Delta k}{k} \approx 10^{-4}$. This produces orbit oscillations around the ring with an amplitude of the order of a few micrometer which is much smaller than the beam size. It is also smaller than other 'natural' orbit oscillations which can not be avoided.

2.3 The Beam Orbit Monitors (BOM)

The beam position is obtained from the beam orbit monitors (BOM). These are attached to almost all quadrupoles in the straight sections and to every second quadrupole in the arcs. They are located at one side of a quadrupole and mounted mechanically on the quadrupole. A schematic cross-section of one type of monitors is shown in Fig. 2.3 (they are slightly different depending on the shape of the vacuum chamber). When a bunch of particles passes, its electrical field induces a signal in the electrodes. This signal is proportional to the bunch current and to the distance between the beam and the electrode. From the four values (corresponding to the four electrodes) one can obtain the beam position independently of the bunch current [Mor].

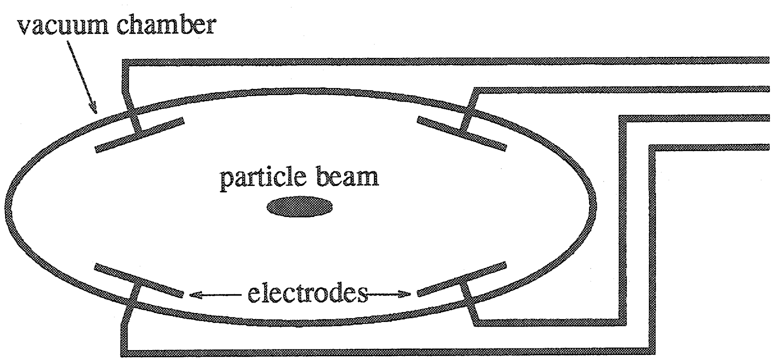

Figure 2.3: Schematic cross-section of an orbit monitor that is used for the position measurements. The electrodes are round with a diameter of 34 mm. The vacuum chamber is elliptic in most parts of LEP. The vertical size of the vacuum chamber is 70 mm, the horizontal 131 mm (in the arcs). The picture is not to scale.

There are two different types of electronics for the monitors. Close to the interaction points electron and positron bunches pass very shortly after each other. Hence the electronics must be fast enough to distinguish between the signals induced by the positron and the electron bunch. These are wide-band electronics which are used for the first four orbit monitors on both sides of the interaction points. To keep the signal in the dynamic range of the electronics one has to use different gains depending on the bunch currents. For the usual bunch currents during luminosity operation the electronics use two different gains (0 dB and 10 dB). All other orbit monitors are equipped with narrow-band electronics which always work with the same gain.

Detailed descriptions of the orbit monitors and both types of the electronics can be found in [Bor93, Bov94, Vis94].

2.4 The Couplers

To detect the small orbit oscillations, two couplers [Vos] are used. Figure 2.4 shows a cross-section of one of the couplers. The electrodes are about 18 cm long. The measurement is more accurate because the electrodes are about five times as large as the electrodes in the orbit monitors and the induced signals are larger. We use the difference signal between two opposite electrodes which is proportional to the bunch current and to the distance of the bunch from the center of the coupler.

The reason for using two couplers is the following. As discussed in the previous chapter (see Eq. 1.29) the amplitude of the oscillation at any point in the ring depends on the β-function at that point and on the phase advance ψ between the observation point and the point where the oscillation is induced. If the argument of the cosine (which depends on the phase advance between

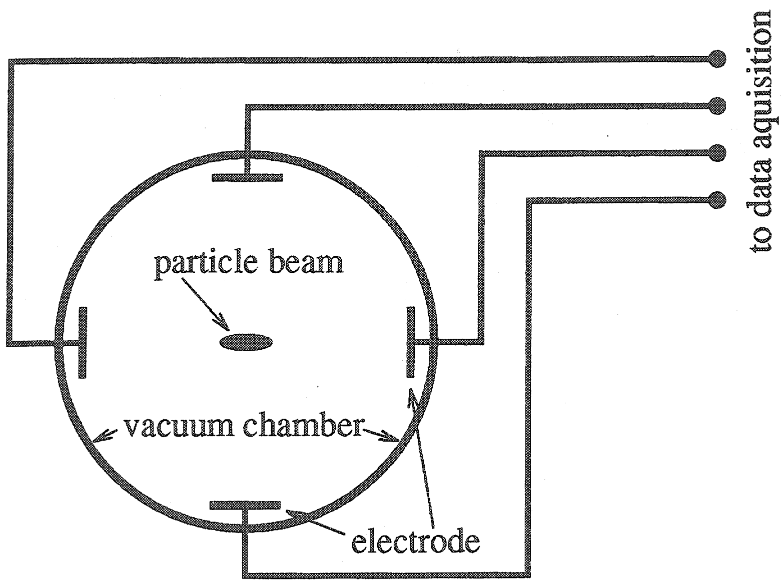

Figure 2.4: Schematic cross-section of one of the couplers. The couplers are installed in the arcs on both sides of interaction point 1 as shown in Fig. 2.5. The diameter of the vacuum chamber in the coupler is 133 mm. The figure is not to scale.

the quadrupole and the coupler) in Eq. 1.29 is close to $\frac{\pi}{2}$ or $\frac{3\pi}{2}$, only the angle of the beam in the coupler changes – but not the position – when the quadrupole strength is changed. The phase advance between the two couplers is no multiple of π ($\Delta\psi_x = 6.24 \cdot 2\pi$ and $\Delta\psi_y = 6.25 \cdot 2\pi$), so we are able to detect any oscillation – wherever it is induced – with at least one of the two couplers. Figure 2.5 shows the location of the two couplers in the LEP-ring.

2.5 The Data Acquisition

The induced orbit oscillations are of the order of 1 μm. To precisely measure their amplitude, the beam position is measured for each bunch passage during a time of almost 40 s: When a bunch travels through the coupler, a signal proportional to the position is measured and the average of either 200 or 400 such signals is recorded. 4096 of these average values are stored in a memory. The amplitude of the oscillations is proportional to the peak height of an FFT-spectrum at the frequency of the modulation. In the following the data acquisition system is described in detail.

The electronics uses existing equipment, which was already installed to test the principle as well as for the first measurements, because no other equipment was available at that time. For the future it is envisaged to develop an improved electronics which is better suited for the data taking.

The electronics for the data acquisition is triggered by a central trigger signal which is distributed around LEP. The trigger signal comes with four times the revolution frequency of LEP (the revolution frequency is 11246 Hz) which gives a distance of about 22 μs between two trigger signals. We use the signal to synchronize a gate with the passage of a particle bunch in the coupler. The signal in the gate is digitized as described below – and shown in Fig. 2.6 – within 15 μs. If LEP is operated with four bunches per particle type we can measure all bunches be-

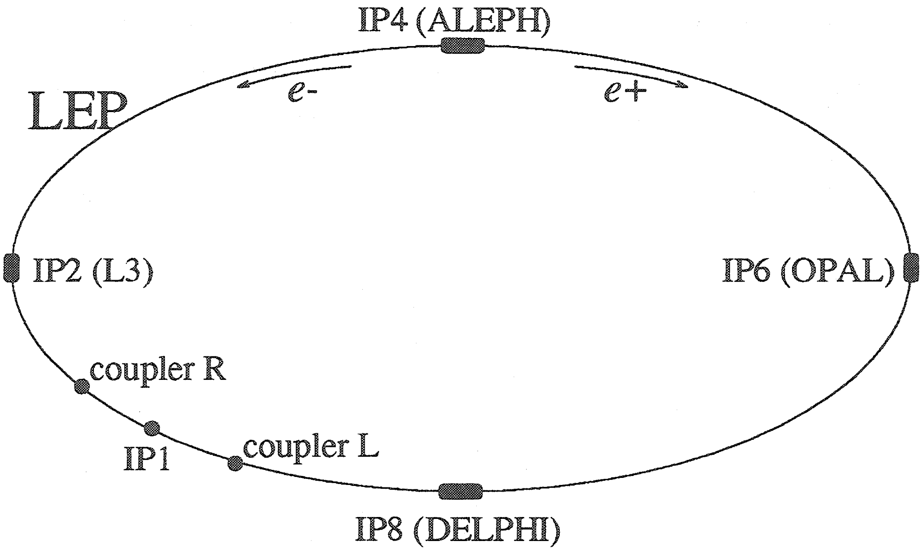

positions of the elements used for the k-modulation

distance between:	
IP2 and coupler R	2370m
IP8 and coupler L	2370m
coupler R and coupler L	1920m
IP1 and couplers	860m

Figure 2.5: Experimental setup for the k-modulation. The quadrupoles that can be modulated are located around the even interaction points. The two couplers are used to detect the induced orbit oscillations.

cause then two bunches of the same particle type are separated by 22 μs. If LEP is operated with eight bunches per particle type (this was the case for most of the time in 1994), we can measure only every second bunch because the distance is only 11 μs.

The eight bunches of electrons and positrons cross at all interaction points and in the middle of the arcs (with four bunches per particle type they only cross at the interaction points). Our two couplers are located symmetrically around interaction point 1 (see Fig. 2.5), so when a positron bunch passes through one coupler at the same time an electron bunch passes through the other one. Therefore the same signal can be used to trigger the acquisition of electrons and positrons. The separation between two bunches is large enough to pose no problems. The signal is the difference signal between the two opposite electrodes; it can be positive or negative depending on the beam position with respect to the center of the coupler.

To digitize the signals they are first integrated in an Integrate/Hold (I/H) which is triggered by the trigger described above. The result from the integration is fed to a 12bit ADC. The digitized result is then read by a digital signal processor (DSP).

The digitization poses two problems:

1. The Integrate/Hold units that are used to integrate the signals can only handle negative signals.

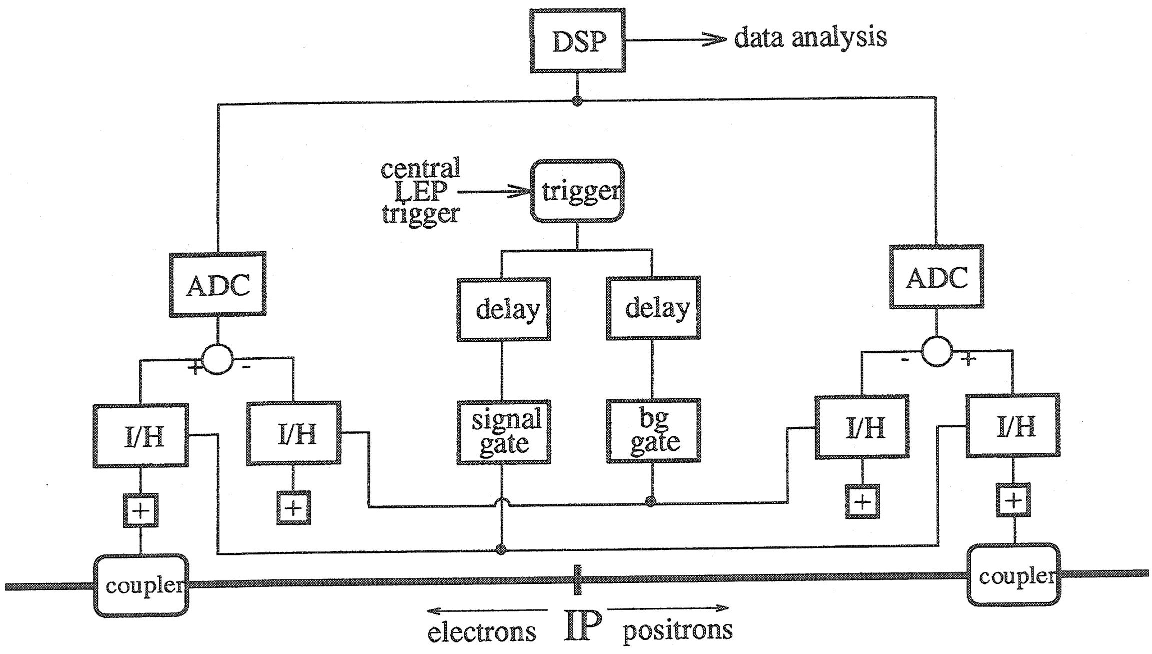

Figure 2.6: Schematic plot of the electronics used to measure the position (one plane only) of the electrons in one coupler and of positrons in the other one. The + are constant currents that are added to the signal. Each of them can be different and has to be adjusted. The second gate (bg) is used to subtract a constant value from the signal that is put into the ADC.

2. The ADCs that digitize the integrated signals can only handle signals in the range between 0 and +5V. Therefore the output of the I/H units has to be in this range.

These problems are solved in the following way: (see also Fig. 2.6). The difference signal for each coupler and each plane is fed into two Integrate/Hold units (one for electrons and one for positrons). The integrated signal is proportional to the beam position. To be able to measure positive and negative signals we subtract a constant current to make the signal negative for the typical positions of the beam. The disadvantage of this is shown in Fig. 2.7.

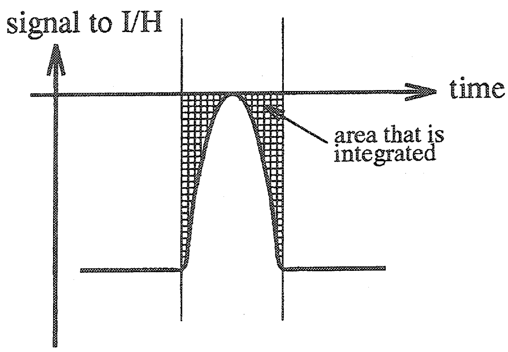

Figure 2.7: The area that is integrated by the Integrate/Hold. The signal shown has the maximum accepted peak height. Therefore the signal (i.e. the integrated area) should be zero.

This reduces the dynamic range of the ADC because the area – and therefore the voltage fed to the ADC – is always greater than zero. To avoid this we subtract a constant voltage from the result with another gate of the same length as the signal gate. The gate comes at a time where no bunch passes through the coupler. The gate is put to another I/H unit on which a constant but adjustable voltage is put as a signal. The output voltage is subtracted from the output of the first I/H and the result is fed to a 12bit ADC. Figure 2.8 shows the signals that go to the ADCs and how they are produced. The linearity of the whole setup is shown in Fig. 2.9.

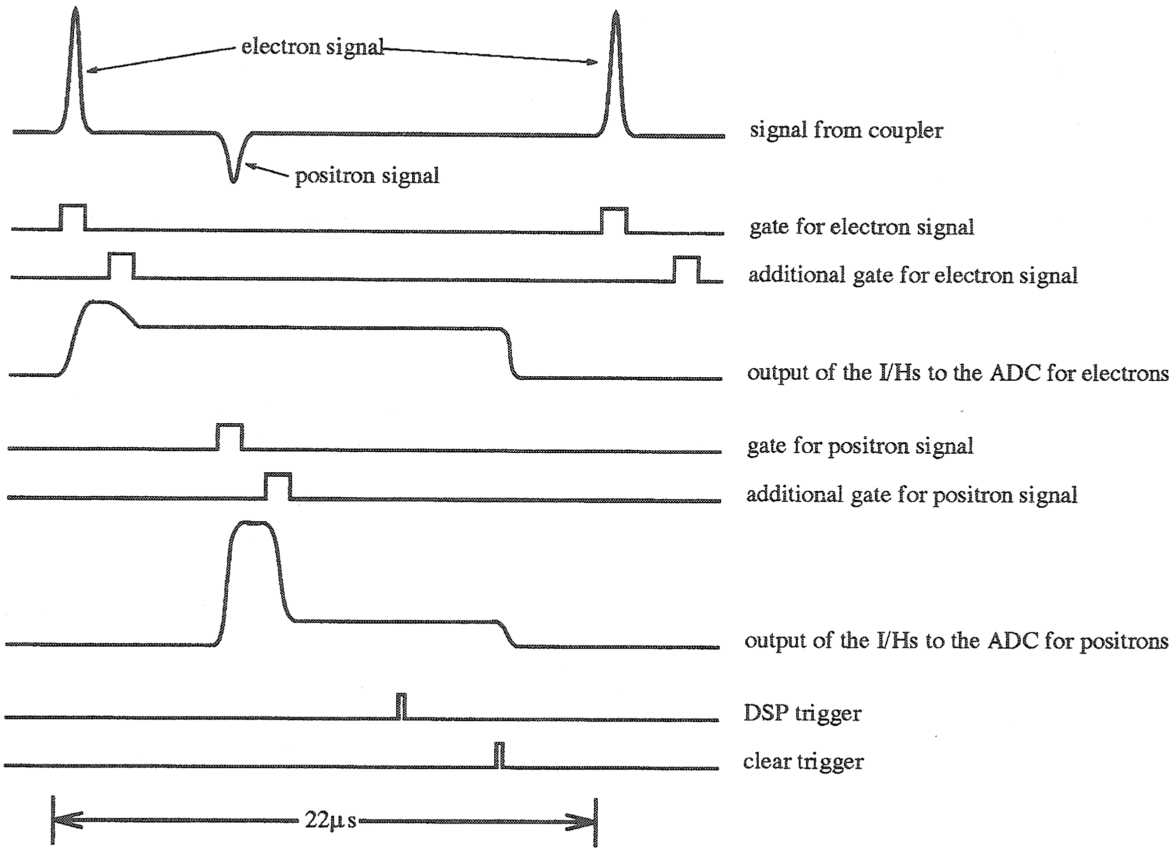

Figure 2.8: Schematic plot of the signals. The length and height of the signals is not to scale.

The signal is proportional to the bunch current. For typical bunch currents in the vertical plane one ADC count corresponds to approximately $\frac{1}{4}$ μm position change. The signals in the horizontal plane are larger, because the beams are about 3 mm away from the center in the horizontal plane[1], which requires a large attenuation before they can be fed into the Integrate/Hold. This leads to a degraded performance (1 ADC count $\approx$ 2 μm).

A Motorola DSP56001 installed in a VME-crate reads out all eight ADC-values and sums over 200 or 400 values per channel. A 68030 microprocessor running the OS9 operating system reads the data from the DSP-memory, divides the sum by 200 or 400 respectively and sends the data to a UNIX-workstation in the LEP control room. The result corresponds to the beam position

[1]This was due to the 'Pretzel' scheme where electrons and positrons were traveling on very different orbits in the arcs. In the running period in 1995 the beams should be nearer to the center so that it will be possible to work with a smaller attenuation.

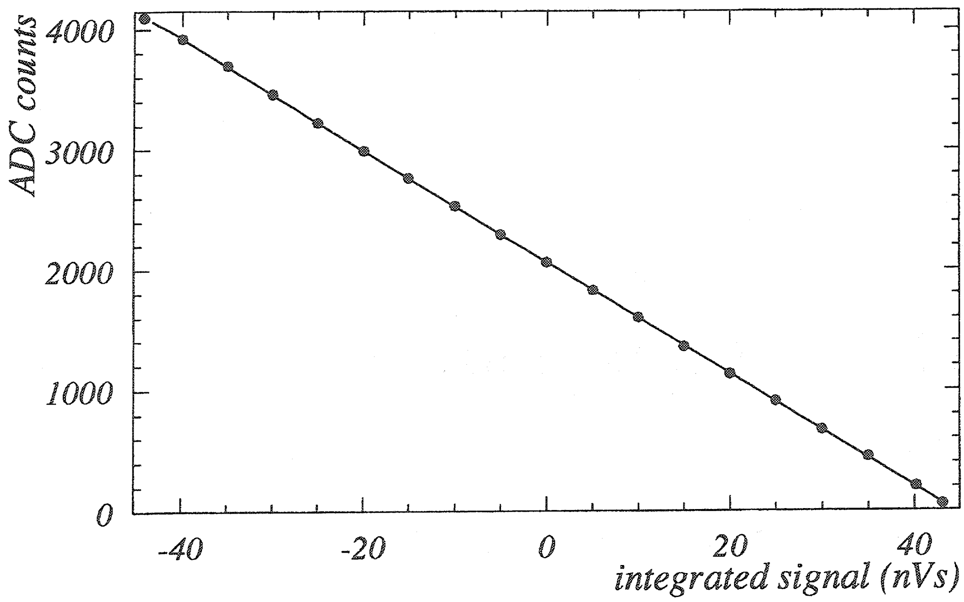

Figure 2.9: Linearity of the electronics. The measurement was done using a pulse generator to produce signals similar to those from the coupler. The integrated signal was measured using a digital oscilloscope. The errors are smaller than the size of the points. The line is the result of a fit.

averaged over 50 or 100 turns and sampling frequencies of 224.92 or 112.46 Hz, respectively. On this workstation two processes are running, one that collects the data from the OS9 and another one that performs the analysis described in the next chapter.

Chapter 3

The Online Data Analysis

3.1 Calculation of the Amplitude

A dataset for one particle type, plane and coupler usually consists of 4096 points. These points correspond to the beam position in the coupler over a period of 18.2 or 36.4 seconds depending on the sampling frequency (224.92 or 112.46 Hz). The frequencies we want to detect are in the range between 0.8 Hz and 15.6 Hz (the revolution frequency of LEP is 11246 Hz).

A discrete Fast-Fourier-Transform (FFT; see Appendix B) is performed on this dataset to obtain the spectrum of frequencies[1] (to obtain the amplitudes one has to sum the squares of the Fourier coefficients and take the square root of the sum). The spectrum is normalized with respect to the beam current of the corresponding particle type because the signal in the coupler is proportional to the beam position and to the bunch current. The normalization with respect to the current allows to be independent of beam current changes (the current decreases with time during a fill). We use the current of all eight bunches of a particle type (usually all bunches have almost equal current) in units of mA for the normalization.

The resulting spectrum gives the amplitudes for the frequencies in ADC counts divided by the current. A typical spectrum with four modulated quadrupoles is shown in Fig. 3.1.

If the beam passes through a modulated quadrupole off center, the beam starts oscillating at the modulation frequency and we expect a peak in the spectrum at this frequency. If the modulation frequency is not stable[2], the frequency can be shifted with respect to the expected frequency.

The amplitude of the signal is obtained by the sum of the FFT-amplitudes at the peak and the two neighboring bins (see Fig. 3.2). The shape of the peak depends on the exact frequency. If the frequency is close to the central frequency of the bin the peak is high and narrow. If the frequency is not centered in a bin the signal is distributed over two bins which leads to a smaller but broader peak (see Fig. 3.3). Simulations have shown that summing over three bins gives results of a sufficient accuracy (the obtained amplitude is higher than the real one, but the linearity is conserved; therefore it does not deteriorate the results). Whenever the amplitude occurs in the following description it means the sum over three bins as described above.

[1] The FFT requires that the number of points is a power of 2. Therefore we use $4096 = 2^{12}$ points.

[2] This was indeed the case for the QS0s and QS1s most of the time of the 1994 running period and caused by the way the modulation was done.

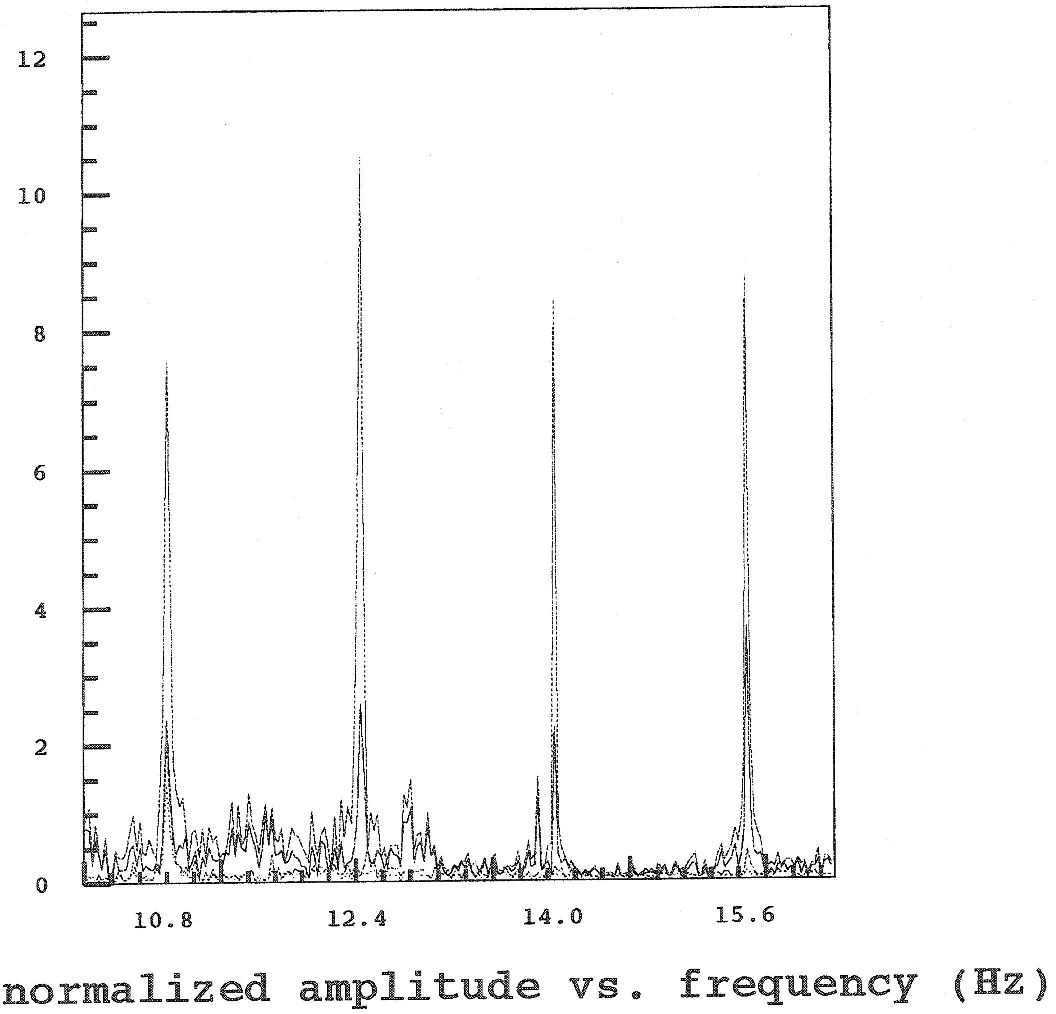

Figure 3.1: FFT-spectra with four modulated quadrupoles (two spectra per plane and two for each particle type). The x-axis gives the frequency in Hz, the y-axis gives the amplitude in ADC counts per mA beam current for the corresponding particle type. The frequencies under the plot give the modulation frequencies. They are located at the places where the peaks are expected. The beam was not centered vertically in the modulated quadrupoles, giving rise to significant peaks in the spectra.

3.2 Storage of the Data

The amplitude, as described previously, is proportional to the beam oscillation amplitude. The amplitude of the beam oscillation is proportional to the distance of the beam from the center of the modulated quadrupole. Therefore we measure the beam position with the beam orbit monitor close to the quadrupole at about the same time as the data for the spectrum is taken. These values (one for each plane and particle type) are stored together with the corresponding measured amplitudes.

The FFT and the peak-finding is done online on a workstation in the LEP-control room. The determination of the offsets, as described in the next chapter, is done off-line. For the 1995 running period it is foreseen to do all the analysis online.

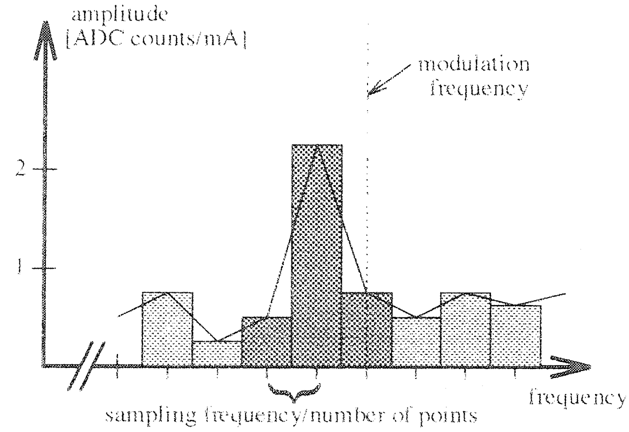

Figure 3.2: Schematic spectrum around the modulation frequency. The three dark bins are summed up to give the amplitude.

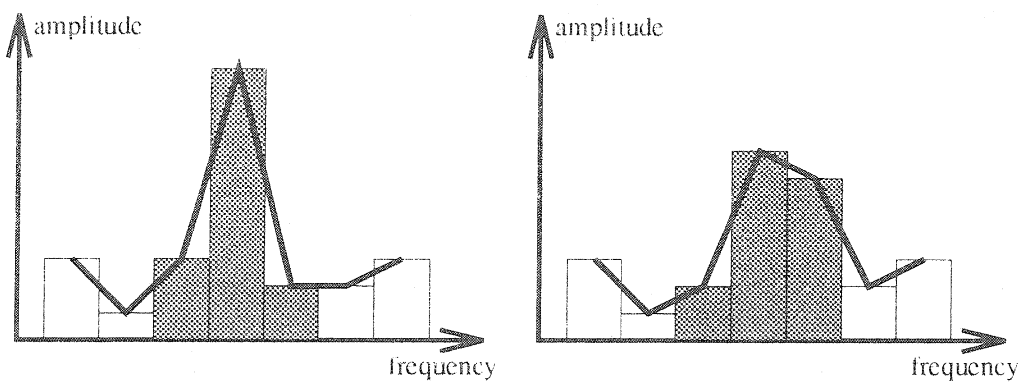

Figure 3.3: These schematic spectra show the reason for the integration. In the left spectrum the frequency is near to the frequency of the bin. In the right one it is almost in the middle between the two bins. If the modulation frequency is not very stable both cases are possible and therefore one has to find a way that gives the same result for both.

Chapter 4

The Offline Data Analysis

4.1 Determination of the Offsets

The offsets of the beam orbit monitors are determined as follows: We continuously record the beam position for the monitor at the modulated quadrupole and the amplitude due to the modulation during a luminosity run for some hours. During this time the orbit drifts are in the order of up to 1 mm (the source of the orbits drifts is not fully understood). When the difference between the measured orbit and a reference orbit becomes to large, the operator performs an orbit correction. Figure 4.1 shows the change of the orbit with time due to orbit drifts and corrections.

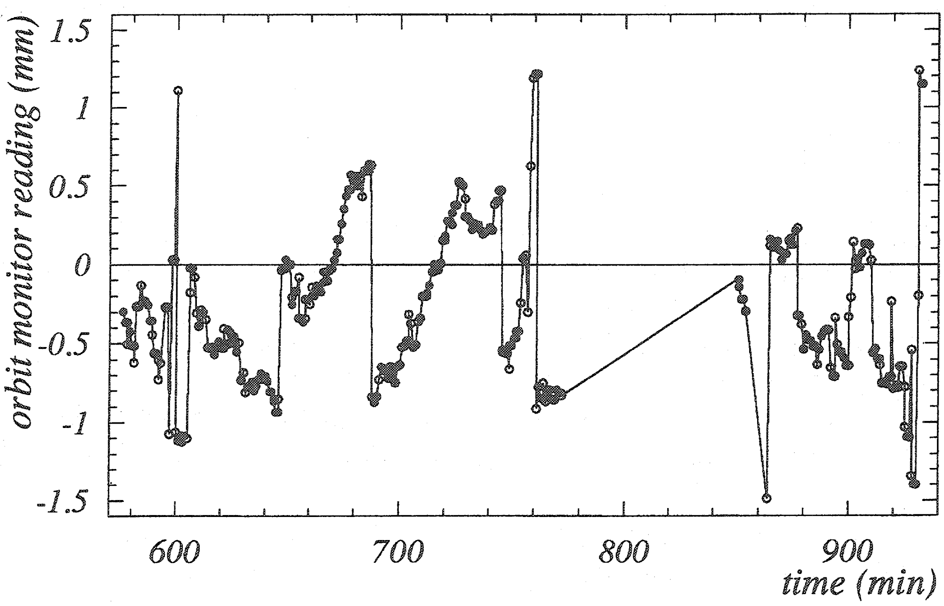

Figure 4.1: Natural orbit drifts and corrections during a luminosity run in a QS0 quadrupole (for the positrons) The fast movements usually are corrections of the closed orbit. The black points are used for the analysis. The white ones are discarded for reasons discussed in chapter 4.2.

To determine the offset, the amplitude is plotted as a function of the orbit monitor reading for values taken at approximately the same time. When the beam passes through the center of the quadrupole, this corresponds to a certain reading of the orbit monitor that we call offset of the monitor. In this case the amplitude is minimum and to both sides the amplitude is expected to rise linearly. Figure 4.2 shows an example for the so-called V-plot.

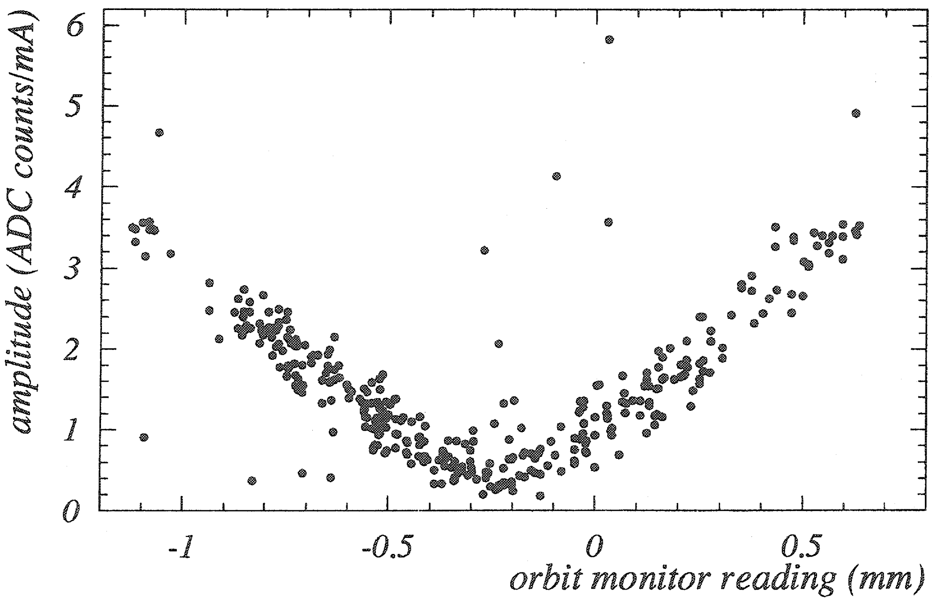

Figure 4.2: V-plot for the positrons at a QS0 quadrupole (vertical). The x-axis is the beam position measured with the beam orbit monitors. The y-axis is the amplitude of the orbit oscillation measured at the corresponding modulation frequency. The point with the smallest amplitude is where the beam is centered in the quadrupole. The data was taken continuously during about 5 hours of a luminosity run.

4.2 Orbit Drifts

Some of the measurements gave results apparently different from the points forming the V-shaped curve. This measurements are related to orbit drifts. The measurement of the spectra is not synchronized with the measurement from the beam orbit monitors which measure approximately every minute. The measurement of the orbit takes about 20 ms. Orbit corrections can lead to beam movements of 500 μm or even more within a few seconds. If we start taking data for a spectrum after the correction and the orbit was measured before the correction, we measure an amplitude that corresponds to a different orbit position than the one previously measured with the monitor.

This is an example of a worst case which does not occur frequently. However, orbit drifts exceeding some 10 μm during the time of the measurement (which can take almost 40 s) are later visible as wrong measurements in the V-plot.

Therefore all measurements are discarded where the orbit changed more than a certain value between two consecutive measurements. In this case both measurements are not used for the analysis.

At the beginning of the 1994 running period we tested different limits for tolerable orbit drifts. The scatter becomes smaller if one uses a lower limit. A cut of 100 μm proved to be very efficient because almost all wrong measurements were discarded but there were enough points left to keep the statistical error smaller than 10 μm for a typical measurement.

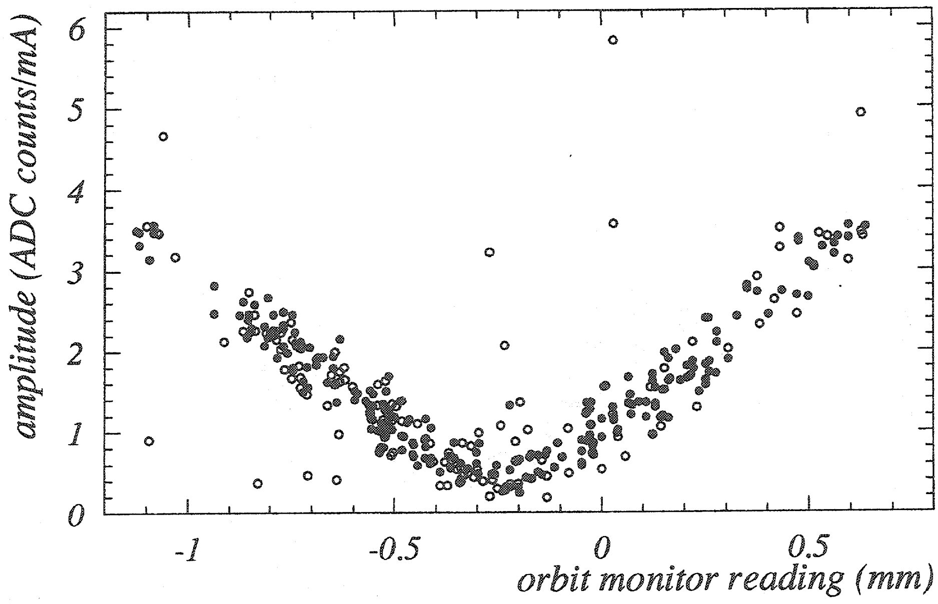

Figure 4.3: V-plot from the same dataset as before. • are good and ∘ are wrong measurements. For a good measurement the orbit drift between two points is less then 100 μm.

Figure 4.3 shows the effect of the cut. The black points are measurements that are still used for the analysis. The white circles are measurements that are left out because the drift of the beam position exceeded 100 μm. Figure 4.1 shows the change of the orbit with time for the same dataset that is used for most of the V-plots in this chapter.

Another effect of orbit drifts is explained in the following : Due to technical reasons the quadrupoles equipped with back leg windings are modulated at frequencies below 2 Hz (see chapter 2.2). Orbit corrections and drifts produce large amplitudes at low frequencies which can be large compared to the amplitudes from the beam oscillations. Therefore the measurement is discarded, if the amplitude in the second bin exceeds a certain value.

Orbit drifts and corrections can also change the beam position in the coupler. The electronics are adjusted such that the average value after the digitization for typical beam positions is between 1000 and 3000 ADC counts. However, if the beam position in the coupler becomes too large, the ADC is saturated and the measurement is not used.

4.3 Offset Calculation Using a Fit

For a rough estimate the offset can be determined from the V-plot by eye. For Fig. 4.2 this yields a value of about -200 μm.

A more accurate value for the offset is calculated by fitting the following function (Fig. 4.4) to the data:

$$A = |(y - P_1) \cdot P_2| + P_3 \tag{4.1}$$

y is the beam position obtained from the beam orbit monitors, A is the amplitude obtained from the spectrum. The parameter P_1 is the offset we want to obtain. P_2 is the slope of the V on one side of the minimum (the slope of the other side is $-P_2$). P_3 is the amplitude at the minimum.

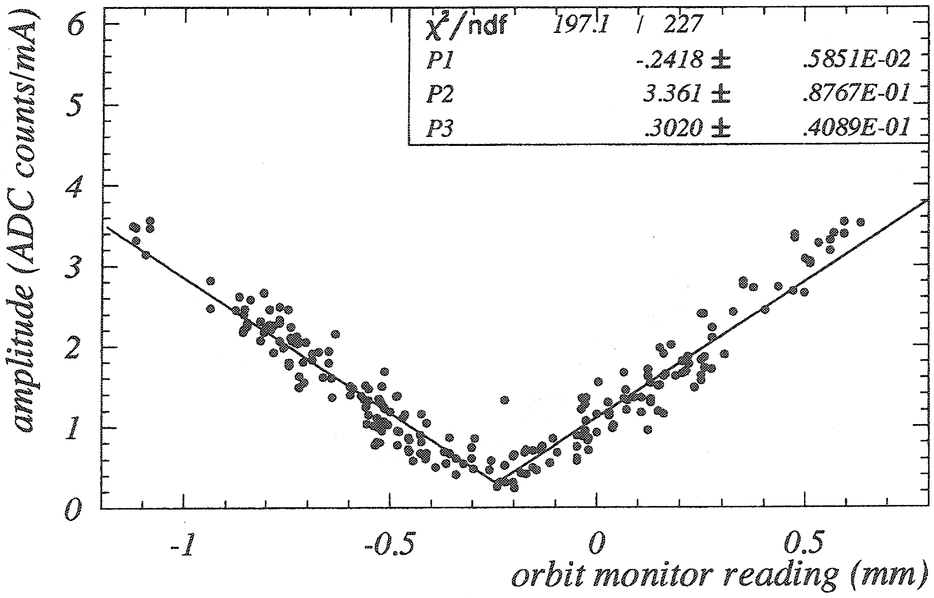

Figure 4.4: This is the same V-plot as in the previous figure. Only good measurements are plotted and used for the fit. The error on the amplitude is 0.3 ADC counts/mA. The offset is $(-241.8 \pm 5.9\mu\text{m})$. The following equation is fitted to the data: $A = |(y - P_1) \cdot P_2| + P_3$. The error is the statistical error of the fit.

This parameter was introduced because noise leads to amplitudes that are always greater than zero.

Due to more than 200 good measurements, corresponding to about five hours of data taking, the error is small. The error on the amplitude is estimated to be about 0.3 ADC counts/mA. The error on the beam orbit monitor reading is smaller than 10 μm [Bov94]. It is not included in the fit. A discussion of the errors will be given later in this chapter (4.5).

4.4 Measurement of Offsets Using Closed Orbit Bumps

Most of the offsets were determined by modulating the strengths of some quadrupoles during luminosity runs and exploiting orbit changes during the run. An alternative method to measure the offset of a monitor is to deliberately displace the beam in the quadrupole with a closed orbit bump (see Appendix C). Figure 4.5 shows an example where a measurement with a closed orbit bump was necessary because the orbit drifts during a fill were too small. This method does not rely on small orbit changes during a long time. Therefore the offset can be determined in 15 to 20 minutes. We choose QS5.R2 to test the monitor calibration by changing the orbit with closed bumps. The modulation of this quadrupole was switched on with an amplitude which was about a factor two higher than the modulation used during parasitic observations. Three measurements with the actual beam position were recorded. Then the beam was moved by 0.5 mm in the center of the quadrupole using a closed orbit bump; again three FFT-spectra were recorded. This procedure was repeated until we had sufficient points on both sides of the minimum to calculate the offset of the orbit monitor. The whole measurement took about 20 minutes. The results are shown in Fig. 4.6.

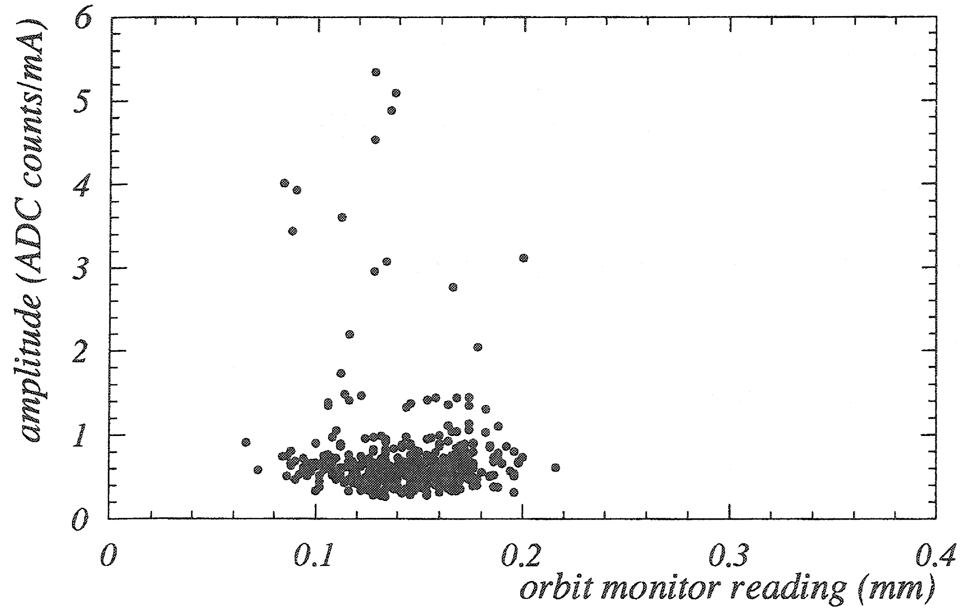

Figure 4.5: V-plot of the electrons in the QS7.L8. The beam moved only by about 100 μm during some hours. It is not possible to obtain a value for the offset. The x-axis is only 0.4 mm compared to about 2 mm in the previous figures. The plot still contains the wrong measurements.

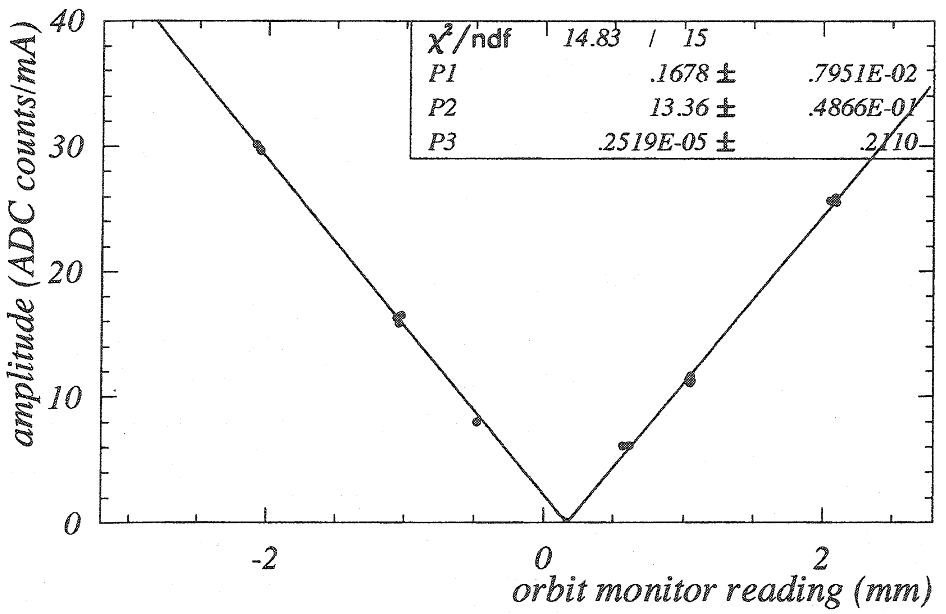

Figure 4.6: Results from the offset calibration with closed orbit bumps, with positrons at QS5.R2. The measurement took about 20 minutes. The error on the amplitude is 0.45 ADC counts/mA. The statistical error of the offset is less than 8 μm.

4.5 Discussion of Accuracy

In the following the accuracy of the measurements is discussed; it depends on:

1. Accuracy of the beam position measured by the monitors.
2. Accuracy of the measured amplitude.
3. Angle of the beam in the quadrupole.
4. Modulation frequency.
5. Misalignments of quadrupoles.
6. Statistical errors.
7. Long-term stability of offsets.

4.5.1 Accuracy of the Beam Position Measured by the Monitors

The reproducibility of the measurements of the beam orbit monitors is about $10\,\mu$m [Bov94]. The absolute values are sometimes strongly biased but can be corrected by our measured offsets. It was expected that the offsets are due to mechanical misalignment between quadrupoles and the orbit monitors. However, different offsets for both particle types and for the different electronic gains were found (see the following chapter). These results can not be explained by a mechanical offset only.

For the determination of the offsets the beam orbit monitor precision is not limiting our measurements. During the measurements of the amplitude – which takes about 40 s – small orbit drifts are unavoidable. The position of the beam at the monitor is measured in a time of about 20 ms. Because both measurements are not synchronized, the orbit measurement does not reflect the average beam position during the measurement of a spectrum. This produces a scatter in the V-plot.

4.5.2 Accuracy of the Measured Amplitude

If we use 4096 values to obtain the spectrum, the distance between two bins is approximately 0.03 Hz (sampling frequency of 112.46 Hz). The frequencies for the modulation of the QS0 and QS1 quadrupoles were not stable during most of the 1994 running period. The summation over three bins reduces the influence from the frequency changes. The amplitude obtained from the summation is higher than the real amplitude which changes the slope of the V curve.

If one modulates two quadrupoles at the same time with frequencies close to each other ($f_1 - f_2 \leq 0.5Hz$), the amplitudes can influence each other (leakage). Simulations which were performed to optimize the analysis of the spectra demonstrated that the summation over three bins proved to be less influenced by leakage from other peaks than other methods that were tested.

The error on the amplitude is different for each quadrupole because the amplitude is different for each quadrupole. The amplitude is proportional to Δk which we can not measure directly and which depends on the frequency. It depends also on the β-function at the quadrupole and on the betatron phase advance ψ between the coupler and the quadrupole. In addition the spectra for the two particle types as well as for the couplers used for our measurements can not be compared, because the electronics used to digitize the signals are different. They use different ADCs and are not adjusted in the same way (see Fig. 2.6).

4.5.3 Angle of the Beam in the Quadrupole

The beam orbit monitors are installed close to the quadrupoles. For the normal-conducting quadrupoles they are mechanically mounted on one side of the quadrupole. The distance between adjacent beam orbit monitor and the superconducting quadrupoles is 44 cm and therefore larger than for other quadrupoles because these quadrupoles are installed in a cryostat, which requires some space.

If the beam passes through the quadrupole center with a large angle, the amplitude of the beam oscillation is small. However, the position of the beam in the monitor is different from a position with the beam passing through the quadrupole center with zero angle (Fig. 4.7). Therefore angle and measured offset are correlated.

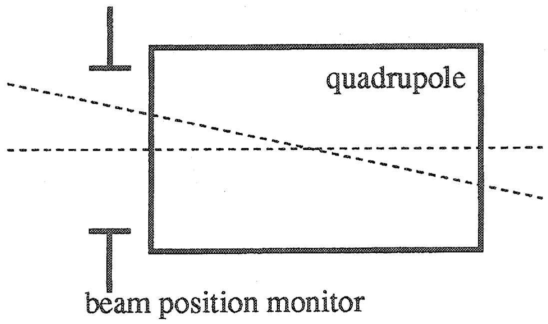

Figure 4.7: If the beam travels through the quadrupole at an angle the oscillation amplitude due to the modulation can be zero. This leads to different offset for different angles. Most of the quadrupoles are 2 m long. The beam position monitor is 17 cm away from one end of the quadrupole. The trajectory inside the quadrupole is approximated to a straight line.

The effect of an angle on the offset can be large, in particular for the superconducting quadrupoles close to the interaction points. When the beams are separated by electrostatic separators to avoid collisions – as during adjustment or energy calibration – the offset differs from the offset measured with colliding beams (during luminosity runs) by 100 to 200 μm. For separated beams the angle in the QS0 quadrupoles is quite large (200 μrad) (see Fig. 4.8). The offset depends on this angle.

Even if the angle is large, the true offset can be found. If the orbit in the adjacent monitor is measured the angle can be estimated. A procedure for the correction using this angle is still under development.

The influence of the beam angle on the offset determination was experimentally studied for one QS10 magnet. The offset was measured for angles of -50, 0 and $+50$ μrad using a closed orbit bump. In normal conditions the angle is one order of magnitude smaller (the excursions due to this angle were approximately 5 mm in some nearby quadrupoles or beam orbit monitors respectively; the RMS of the whole closed orbit during luminosity runs is of the order of 0.5 mm). The measured dependence of the offset on the angle is shown in Fig. 4.9. The typical systematic

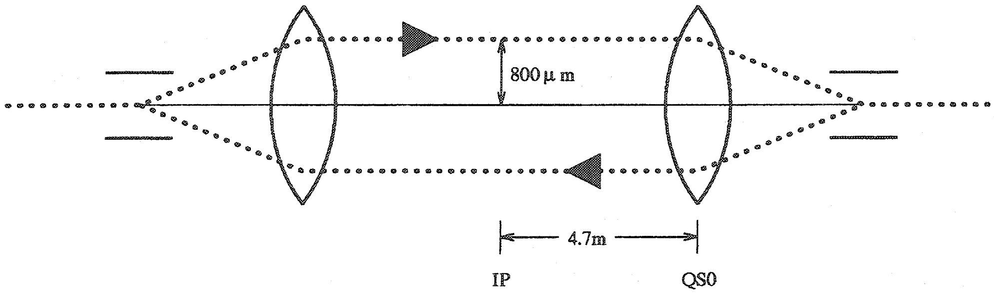

Figure 4.8: Electrostatic separators separate the two beams vertically at the interaction point to avoid collisions (e.g. during adjustment or energy calibration). The angle in the QS0 quadrupoles is much larger than the angle during collisions.

error on the offset from an angle in the quadrupole magnet is calculated from the measurements. The error is about $3\frac{\mu m}{\mu rad}$. A typical closed orbit at a place with no large deviations has an RMS of about 500 μm. For a distance of 50 m between two quadrupoles this would lead to an angle of 10 μrad. This yields a systematic error due to the angle of 30 μm (this is only true if there are no large orbit excursions close to the quadrupole).

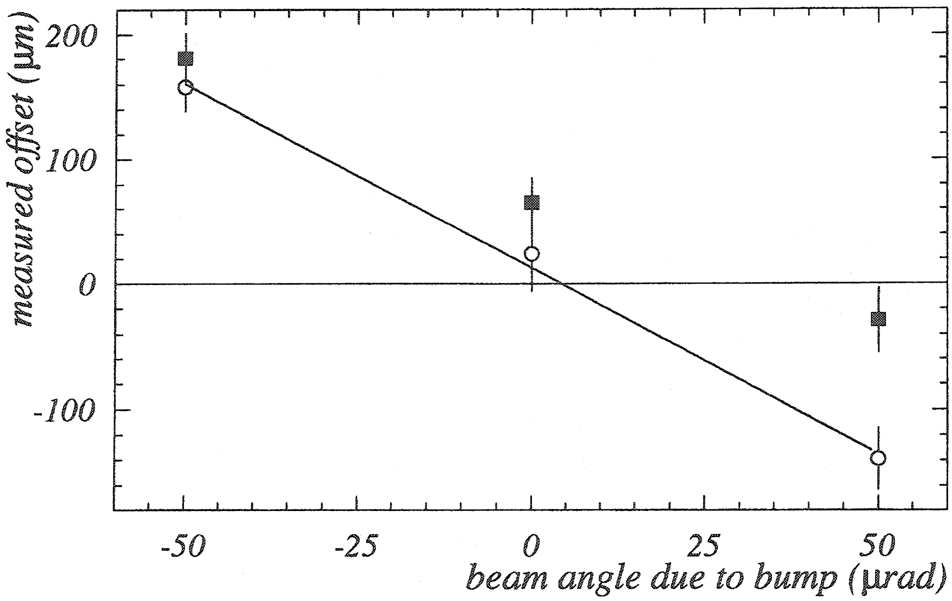

Figure 4.9: Results from the measurements for QS10.L2 to determine the influence of the angle. The offsets are preliminary results. The open circles are the values for the positrons, the black squares those for the electrons. An angle of 1 μrad changes the offset by approximately 3 μm.

4.5.4 Modulation Frequency

An effect of the modulation frequency on the offset is not expected. However, the choice of the frequency determines the value of the slope of the V shaped curve, because the modulation of the magnetic field in the vacuum chamber depends on the frequency due to the inductance of the magnet and eddy currents in the vacuum chamber walls. This was measured by using different frequencies for the same quadrupole during one fill. For every frequency we recorded data during one or two hours. As expected, the slope of the V shaped curve which is proportional to Δk was lower for higher frequencies (see Fig. 4.10).

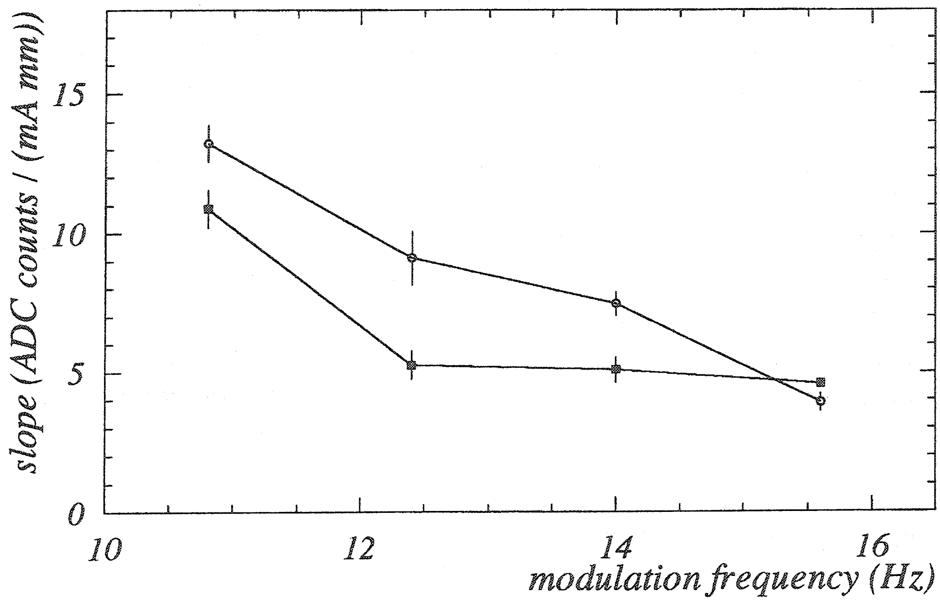

Figure 4.10: Preliminary results for the dependence of the slope of the V shaped curve on the modulation frequency. The circles give the values for electrons the squares the positrons. All measurements were done during the same fill for the quadrupole QS0.R2. The errors are only the statistical errors from the fit. The frequencies are the same as for most of the other measurements.

One mechanism can lead to different offsets for different frequencies: If due to an external source the beam is already oscillating at the modulation frequency, the oscillation amplitude due to modulation of the quadrupole strength is modified. If the oscillation of the beam has a constant phase with respect to the modulation frequency this will displace the V shaped curve sideways and therefore result in a wrong offset. This effect is smaller than other errors because in the analysis of the measurements mentioned above we did not observe any significant dependence of the offset on the frequency.

4.5.5 Misalignments of Quadrupoles

Misalignment of a quadrupole does not affect the results of the measurements of the offsets, since the relative position of the center of the orbit monitor with respect to the center of the magnetic field is measured. If all monitor offsets in a straight section are known, it will be possible to extract the misalignment of the quadrupoles. One of the reasons for developing the k-modulation technique was to provide means of determining such misalignments [RSch93].

4.5.6 Statistical Errors

If the offset is determined by fitting a function to the data as explained above (see Fig. 4.4), the statistical error is smaller than 10 μm. This error is smaller than the error of the orbit monitors or the dependence of the offset on the angle of the beam in the quadrupole.

The accuracy of the results of the FFT can be improved by taking more measurements per dataset. This results in a better resolution of the peaks if the frequencies are close together. We usually take 4096 measurements, which gives peaks in the spectrum with a width of one bin. This resolution is sufficient. Increasing the number of measurements by a factor of two is not expected to improve the results because the time for one measurement – more than 70 seconds – becomes too long. Typically the orbit in LEP is not stable enough to measure such a long time.

4.5.7 Long-term Stability of the Offsets

The offsets depend on the calibration of the orbit monitors which is done after almost every fill. The offset of a monitor close to one quadrupole near IP 2 was measured 11 times during a period of 150 days. The results from this measurements are shown in Fig. 4.11. The offset of this monitor is very small. The measured differences can be explained by the systematic errors discussed above, as the dependence of the offset on the beam angle or re-calibration of the orbit monitor system.

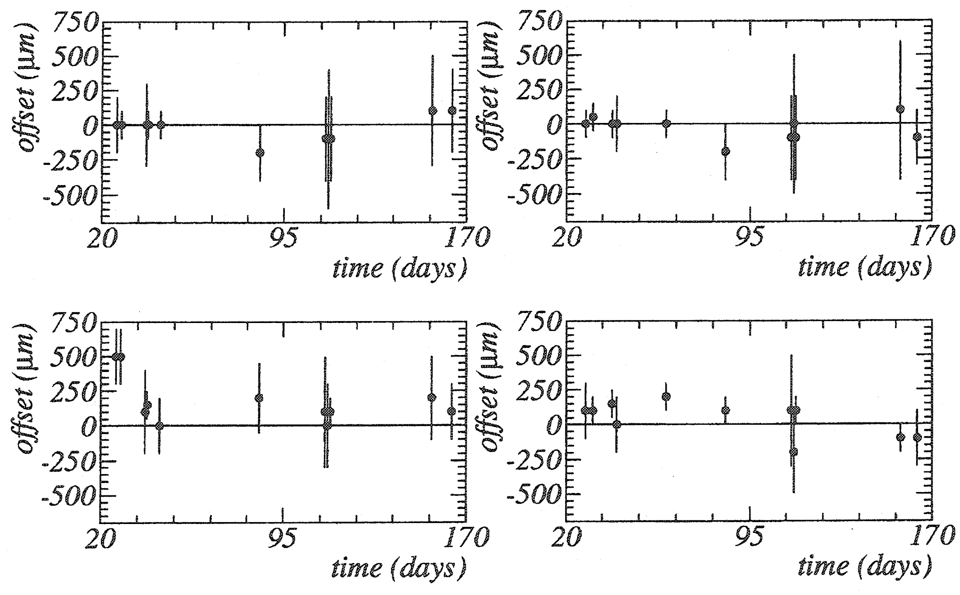

Figure 4.11: Long-term stability of measured offsets for one monitor close to IP2. The top row the offsets for the electrons, the bottom row the offsets for the positrons. On the left side the data for gain 0dB are shown, on the right side the data for gain 10dB.

Figure 4.12 shows the distribution of the measured offset compared to the mean value. All values are from the same quadrupole but from different gains and both particle types. The mean value was calculated for each particle type and each gain to be able to compare the results. The variation includes changes due to the calibration of the orbit monitors and all errors due to our measurement technique.

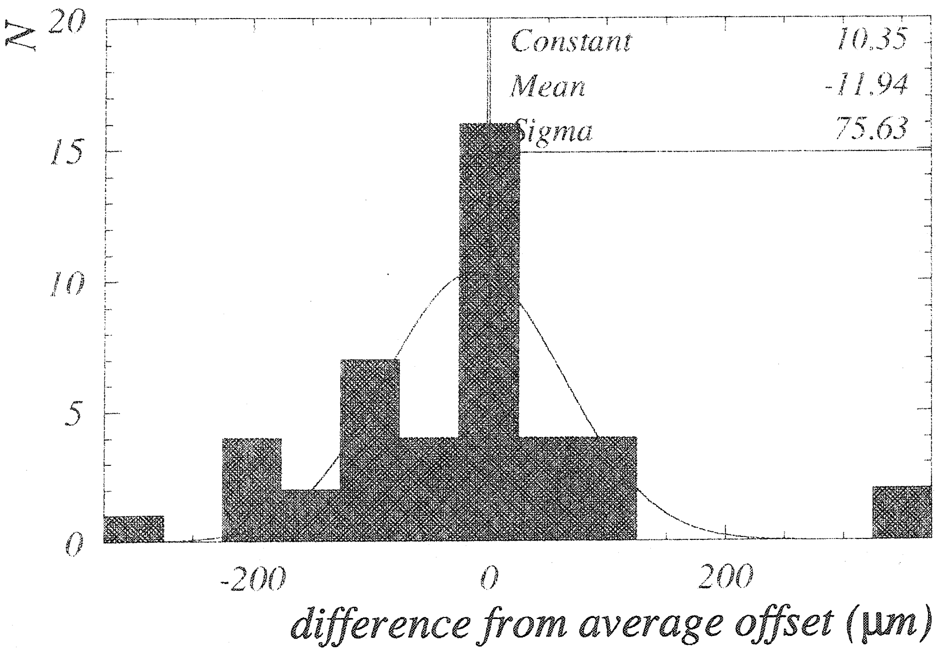

Figure 4.12: Distribution of the measured offsets for one orbit monitor as in Fig. 4.11. The values are the difference of the offset to the average offset for the corresponding particle type and gain.

4.6 Accuracy of Offsets

We are able to determine the offsets with an accuracy of 100 μm or less if we have sufficient data on both sides of the V shaped curve. If the recorded data shows only one side of the V shaped curve the error on the offset becomes larger. Influences from frequencies and from the beam angle are still under investigation, but it is envisaged to reduce the error to less than 50 μm. The statistical errors are much smaller. As we can not determine the influence of the angle exactly, the values given in the table are estimates.

angle	30 μm
frequency	10 μm
amplitude & statistic	10 μm
reproducibility of BOM	10 μm
long-term stability of BOM	unknown
long-term stability of measured offsets	75 μm

Table 4.1: Errors on offsets.

Chapter 5

Results

5.1 Offsets of the Beam Orbit Monitors

During the 1994 running period the offsets of all orbit monitors close to the QS0 and QS1 quadrupoles were measured, as well as the offsets of some other monitors, in particular around interaction point 8. From the results we could compare the offsets of the monitors close to the superconducting quadrupoles to those close to the normal conducting quadrupoles. We were also able to compare the offsets for monitors equipped with wide and narrow-band electronics (see chapter 2.3).

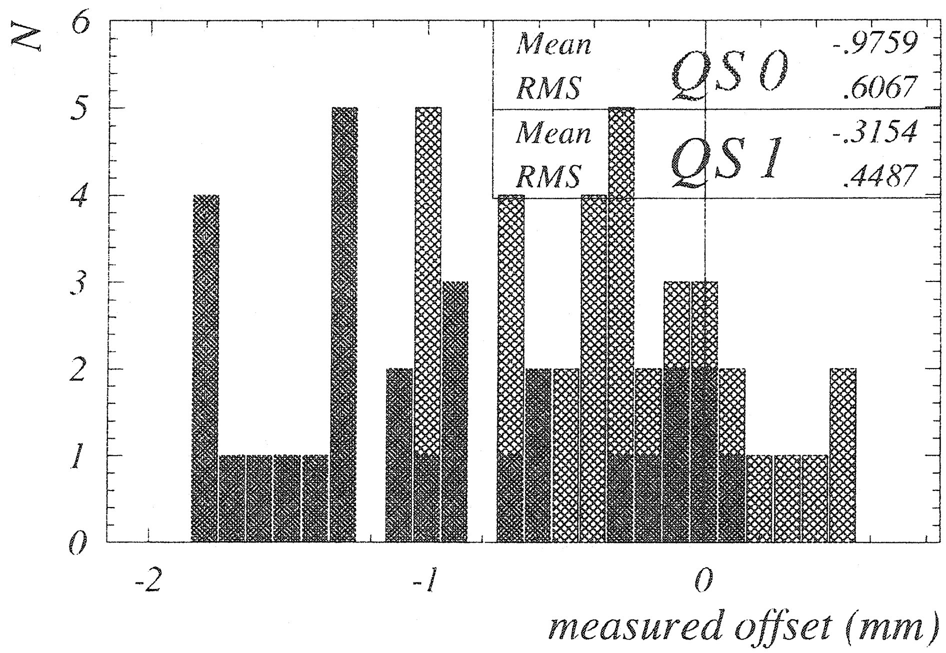

Figure 5.1: Distribution of the offsets of the wide-band orbit monitors. The darker columns mark the QS0s, the lighter ones the QS1s.

For the monitors with wide-band electronics, the results from the monitor calibration with k-modulation yielded different offsets for both particle types as well as for different gains. The reason for the difference is not fully understood, but is likely due to the electronics and the calibration of the monitors which is quite complex and might well produce such effects

[Cocq91, Mor]. In normal luminosity conditions only two gains settings are used (0 dB for currents > 220 μA / bunch and 10dB for currents < 220 μA / bunch).

The monitors close to the superconducting quadrupoles (QS0) have the largest offsets with a mean value of -976 μm (Fig. 5.1). For monitors with wide-band electronics close to normal conducting quadrupoles the offset is much less. Therefore we assume that the large offsets for the monitors close to the QS0 quadrupoles are mainly caused by mechanical misalignment between the quadrupole and the orbit monitor.

The narrow-band monitors have much smaller offsets. This can be seen from Fig. 5.2. The RMS is less than 250 μm.

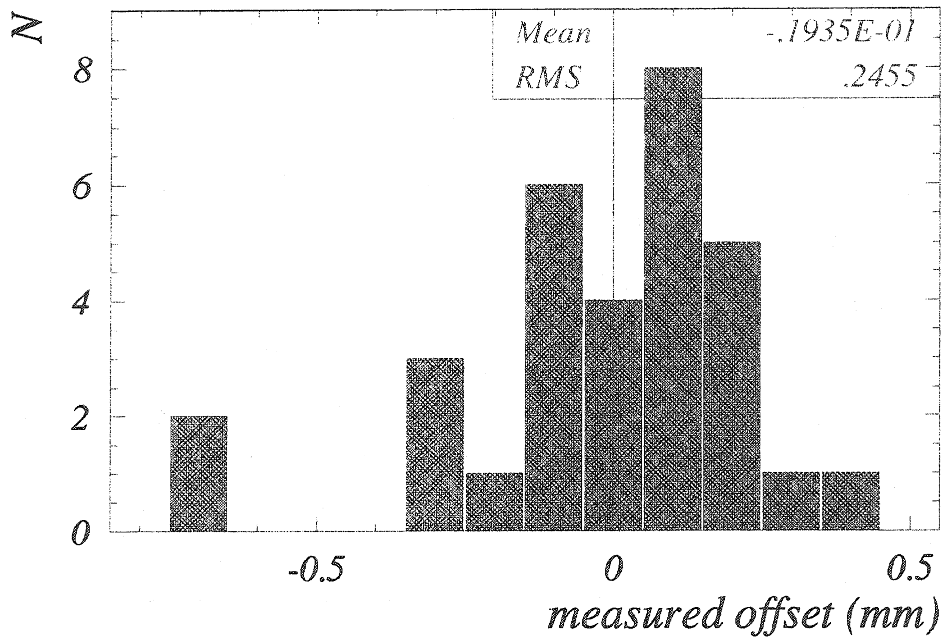

Figure 5.2: Distribution of the offsets of the narrow-band orbit monitors.

The values for the offsets are given in appendix A. Tables A.1 and A.2 contain the offsets for the wide-band monitors. Table A.3 gives the values for the narrow band monitors.

5.2 The 'Golden Orbit'

The offsets for the QS0 and QS1 quadrupoles have been included in the software that retrieves the orbit from the raw data of the orbit monitors. The orbit is calculated and as a final step the offset is subtracted. The data structure allows only two offsets (one for each plane) to be included for each monitor. Therefore we use an average over the different values for the gains and particle types.

To optimize the luminosity, the orbit is corrected towards a reference orbit called the 'Golden Orbit' (see chapter 1.6). Without correcting the monitor readings for the offsets the measured orbit in the straight sections can not be produced by the installed magnets. In Fig. 5.3 the quadrupoles are shown as lenses. A typical vertical orbit which is off center in the quadrupoles is drawn. Figure 5.4 shows the 'Golden Orbit' around the interaction points with and without the offsets. The measured orbit after the offset correction has the same structure as the orbit in Fig.

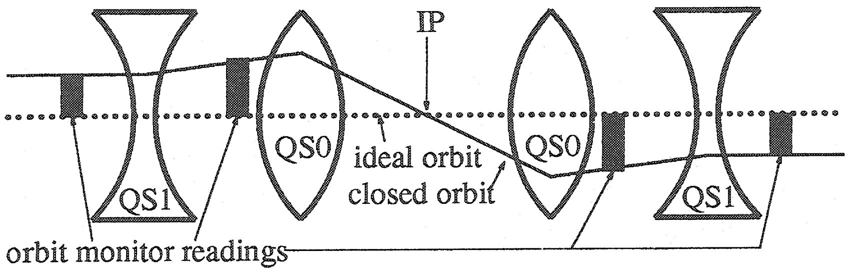

Figure 5.3: Schematic plot of the vertical orbit around the interaction point (IP) if it is not centered in the quadrupoles. The quadrupole strengths and distances are arranged such that the orbit is asymmetric around the interaction point.

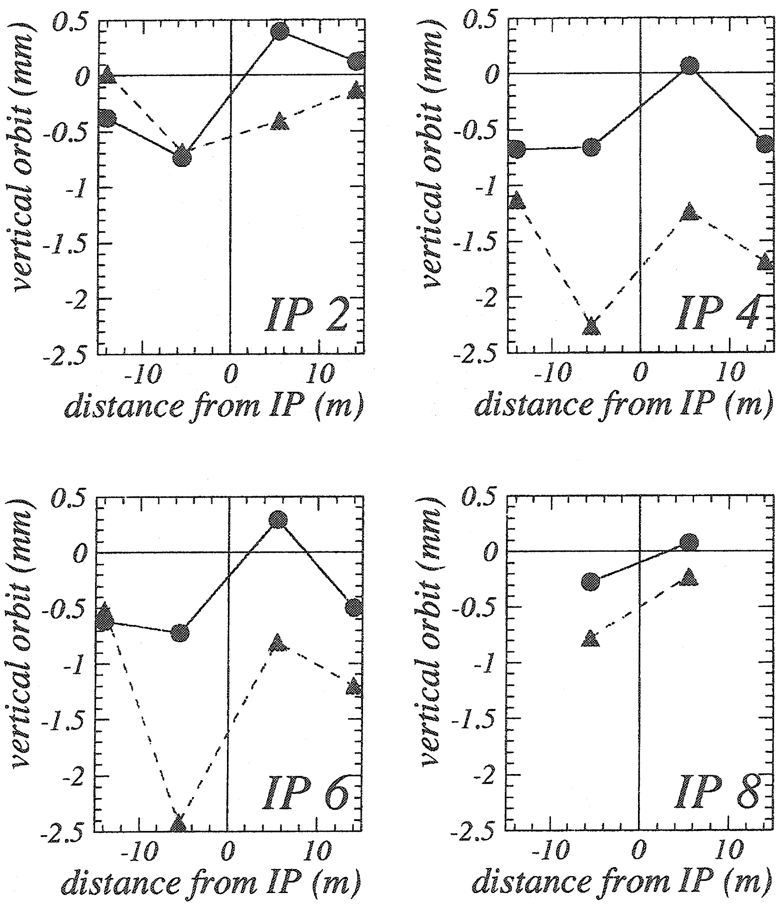

Figure 5.4: The vertical 'Golden Orbit' at the even interaction points. The triangles mark the 'Golden Orbit' before offset correction and the circles are the corrected readings. The two points close to the center are the readings for monitors at the vertically focusing QS0 quadrupole, the outer points are the readings of the monitors at the vertically defocusing QS1 quadrupoles. Two orbit monitors around IP8 were disabled.

5.3. whereas the orbit through the straight section without offset correction cannot be produced by the installed magnets, even if large values for the misalignment are assumed.

Before the offsets were measured, the readings from the wide-band orbit monitors were discarded in the software to calculate orbit corrections. That made orbit corrections close to the interaction point difficult.

5.3 Side Effects of k-Modulation

Most of the measurements were performed during normal luminosity runs of LEP. This is only possible if the measurements do not influence any machine parameters significantly. At the start of the running period in 1994 we modulated only one quadrupole with a very low amplitude. Later we modulated up to eight quadrupoles at the same time, some of them with increased excitation amplitudes. We did not observe any adverse effect on the luminosity and the background in the four LEP-experiments.

As mentioned in the first chapter, the modulation of the quadrupole strength changes the betatron-tunes. The change does not affect the performance of the machine. Yet we could measure this change using the instrument that is measuring the tunes (Q-meter): When we were modulating some quadrupole strengths there was a scatter in the measured tune of the order of $\delta Q = 0.001$. Without the modulation, the scatter disappeared. This has no adverse effects on the normal operation of the machine. Only for very accurate tune measurements (e.g. to measure the coupling between the horizontal and the vertical betatron-oscillations), the quadrupole strength modulation must be switched off, because effects of the order of $\delta Q = 0.0001$ are to be measured.

When we modulated the quadrupole strengths with a three times higher amplitude at low frequencies (those < 2 Hz) we observed an obvious influence on the measured beam size. The time dependence of the beam-size measured with a UV light telescope displayed our modulation frequency of 0.8 Hz when we used the highest possible modulation amplitude. With the amplitudes that we use normally the effect is not visible.

5.4 Further Usage

Another motivation to measure the offsets of the orbit monitors as precisely as possible is the requirement to calibrate the LEP beam energy: the energy calibration is done by resonant depolarization [ECAL] which requires a high level of transverse spin-polarization. A high degree of polarization is obtained, if the beam passes through the arc quadrupoles on an orbit close to the centers of the magnets.

The technique that is used to optimize the polarization (HSM) requires an exact measurement of the orbit in the arc quadrupoles [Ass94]. Figure 5.5 shows the influence of the monitor offsets on the achievable polarization level [Cham95]. Until now the hardware to modulate the strengths of these quadrupoles is not installed. The orbit monitors in the arcs are equipped with the same electronics as the narrow-band monitors in the straight sections. Therefore we expect the offsets to be in the same range. Before the systematic measurements with the k-modulation were done the offsets were expected not to exceed 200 μm. The RMS of the offsets of the narrow-band monitors so far measured is about 250 μm.

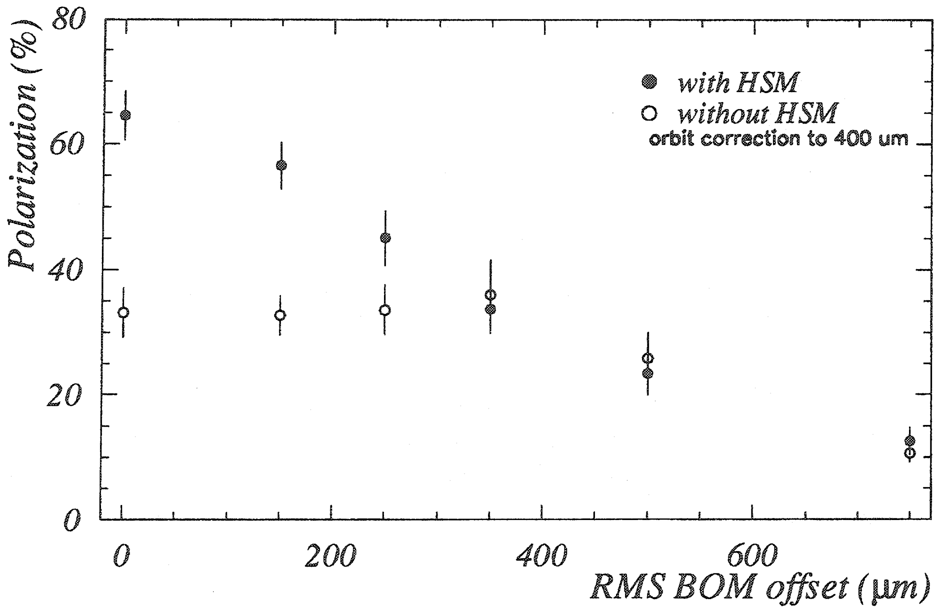

Figure 5.5: Simulation of the influence of offsets on the polarization level and the improvement of the polarization level by harmonic spin matching (HSM).

Conclusion

With the k-modulation technique the position of a particle beam with respect to the magnetic center of a quadrupole can be measured. It is therefore possible to determine the orbit monitor offset, which is the monitor reading when the beam travels through the magnetic center of the adjacent quadrupole. The offsets of more than 25 orbit monitors were determined during the LEP 1994 running period.

Modulating the strengths of up to eight quadrupoles at the same time with $\frac{\Delta k}{k} \approx 10^{-4}$ has no adverse effect on the performance of LEP. The only measurable influence are small tune changes ($\delta Q \approx 0.001$) which do not influence the operation of the machine.

Two methods to measure the offset of an orbit monitor were developed :

- During a fill the orbit changes due to natural drifts and orbit corrections by the operator. The amplitude of the oscillations due to the quadrupole strength modulation is recorded together with the beam orbit monitor reading. From the data the monitor reading for vanishing oscillation amplitude – the offset – is extracted.

- Another method does not rely on orbit drifts during a fill : The beam is moved to different positions in the quadrupole using closed orbit bumps. Again, from the data of the beam orbit monitors and the oscillation amplitude the monitor offsets can be calculated.

The statistic error of the offset measurement is in the order of 10 μm or less, and therefore small compared to the systematic error.

The main contribution to the systematic error comes from the angle of the beam in the quadrupole. This error is expected to be less than 30 μm for orbits with no large excursions (less than 1 mm) close to the position monitor and quadrupole where the offset is to be determined.

During the 1994 running period the offsets of all monitors at the QS0 and QS1 quadrupoles at the even interaction points have been measured. The offsets were much larger than expected and a dependence of the offsets on the gain of the orbit monitor electronics was found as well as different offsets for both particle types. In addition the offsets of other monitors around interaction point 8 were measured.

At LEP, the technique to optimize the luminosity is to correct the orbit to a so-called 'Golden Orbit'. In particular around the interaction point this orbit has large excursions, and the displacements at the monitors can not be understood by quadrupole misalignments.

After the calibration of some of the beam orbit monitors the offsets of the monitors could be subtracted in the 'Golden Orbit': The measured excursion of the 'Golden Orbit' became much smaller, and the beam displacements are not any longer in contradiction with assumptions about machine misalignments.

Appendix A

Offsets

Comments on the Tables

These are the results of the measurements performed during the 1994 running period of LEP. Each of them is the result of a measurement during one fill. The offsets are estimated by eye from the V-plots because for many quadrupoles we had only data on one side of the V-shaped curve. For these V-plots the offset calculation using a fit does not give any sensible results.

	gain	e^-	e^+
QS0.L2	0dB	100 ± 100	0 ± 50
	10dB	-100 ± 100	-100 ± 50
QS0.R2	0dB	-700 ± 100	-900 ± 50
	10dB	-950 ± 100	-900 ± 100
QS0.L4	0dB	-1450 ± 100	-1550 ± 100
	10dB	-1650 ± 100	-1750 ± 50
QS0.R4	0dB	-1250 ± 100	-1375 ± 50
	10dB	-1300 ± 100	-1350 ± 100
QS0.L6	0dB	-1700 ± 100	-1800 ± 50
	10dB	-1850 ± 100	-1775 ± 50
QS0.R6	0dB	-1100 ± 100	-950 ± 50
	10dB	-1300 ± 50	-1125 ± 50
QS0.L8	0dB		-650 ± 100
	10dB	-300 ± 100	-650 ± 100
QS0.R8	0dB		0 ± 100
	10dB	-200 ± 100	-250 ± 100

Table A.1: Vertical offsets of the wide-band orbit monitors for the QS0s (superconducting).

	gain	e^-	e^+
QS1.L2	0dB	450 ± 50	350 ± 50
	10dB	300 ± 100	450 ± 100
QS1.R2	0dB	-200 ± 100	-275 ± 50
	10dB	-225 ± 50	-300 ± 50
QS1.L4	0dB	-300 ± 100	-450 ± 100
	10dB	-425 ± 50	-500 ± 50
QS1.R4	0dB	-1050 ± 100	-1050 ± 100
	10dB	-1050 ± 100	-1050 ± 100
QS1.L6	0dB	50 ± 100	200 ± 100
	10dB		
QS1.R6	0dB		
	10dB		
QS4.L8	0dB		
	10dB	0 ± 150	350 ± 150
QS1.L8	0dB		
	10dB	-400 ± 50	-425 ± 50
QS1.R8	0dB		
	10dB		-300 ± 50
QS4.R8	0dB		
	10dB	175 ± 50	-500 ± 50

Table A.2: Vertical offsets of the wide-band orbit monitors at normal conducting quadrupoles.

	e^-	e^+
QS10.L2	-100 ± 50	-100 ± 50
QS5.L2	200 ± 100	250 ± 100
QS5.R2	150 ± 100	200 ± 100
QS8.R2	100 ± 50	50 ± 50
QS12.L4	150 ± 100	125 ± 50
QS12.L8	-100 ± 200	-500 ± 100
QS11.L8		
QS10.L8	25 ± 50	150 ± 50
QS9.L8	-300 ± 100	-300 ± 100
QS8.L8	150 ± 100	-50 ± 100
QS7.L8	-75 ± 70	-50 ± 70
QS6.L8	200 ± 100	50 ± 100
QS5.L8		-250 ± 50
QS5.R8	225 ± 50	
QS6.R8		0 ± 50
QS7.R8	-1000 ± 150	-1000 ± 150
QS8.R8		
QS9.R8	-50 ± 50	0 ± 50
QS10.R8		
QS11.R8		
QS12.R8	-100 ± 100	0 ± 100

Table A.3: Vertical offsets of the narrow band orbit monitors. Most of the time we could only measure around interaction point 8. The power-converters for the other straight sections were only installed about three weeks before the end of the 1994 running period. Therefore we have only very few measurements for the other straight sections.

Appendix B

Fast-Fourier-Transform (FFT)

This is the FORTRAN-subroutine that is used to calculate the FFT. It is taken from [FFT].

```
      SUBROUTINE FFT(hlist,numlist)

C
C     This routine calculates the FFT of the data contained in hlist.
C
C     hlist ist expected to be double precision!
C
C     numlist has to be a power of 2, otherwise the routine will NOT work!!!
C
C     hlist must contain numlist complex numbers in the following way:
C     hlist(1) is the real part of the first point
C     hlist(2) is the imaginery part of the first point
C     hlist(3) is the real part of the second point and so on.
C
C     The FFT is returned in the same way (so the original data is lost!!!)
C

      INTEGER numlist,i,j,m,mmax,istep
      REAL*8  hlist(40000)
      REAL*8  tempr,tempi
      REAL*8  theta,wpr,wpi,wr,wi,wtemp

      j = 1
      n = 2*numlist
      DO 20 i = 1,n,2
         IF (j .GT. i) THEN
            tempr      = hlist(j)
            tempi      = hlist(j+1)
            hlist(j)   = hlist(i)
            hlist(j+1) = hlist(i+1)
            hlist(i)   = tempr
            hlist(i+1) = tempi
         ENDIF
         m = n/2
 10      IF ((m .GE. 2) .AND. (j .GT. m)) THEN
            j = j - m
            m = m/2
            GOTO 10
         ENDIF
```

```
         j = j + m
 20    CONTINUE
       mmax = 2
 30    IF (n .GT. mmax) THEN
         istep = 2*mmax
         theta = 6.28318530717959D0/DBLE(mmax)
         wpr   = -2.D0*DSIN(.5D0*theta)**2
         wpi   = DSIN(theta)
         wr    = 1.
         wi    = 0.0D0
         DO 50 m = 1,mmax,2
            DO 40 i = m,n,istep
               j          = i + mmax
               tempr      = wr*hlist(j) - wi*hlist(j+1)
               tempi      = wr*hlist(j+1) + wi*hlist(j)
               hlist(j)   = hlist(i) - tempr
               hlist(j+1) = hlist(i+1) - tempi
               hlist(i)   = hlist(i) + tempr
               hlist(i+1) = hlist(i+1) + tempi
 40         CONTINUE
            wtemp = wr
            wr    = wr*wpr - wi*wpi + wr
            wi    = wi*wpr + wtemp*wpi + wi
 50      CONTINUE
         mmax = istep
         GOTO 30
       ENDIF

       END
```

Appendix C

Closed Orbit Bumps

Closed orbit bumps change the position of the beam only in a small part in the ring where it is desired but leave it undisturbed in the rest of the ring.

For our measurements we used two different types of closed orbit bumps. Most of them were used to reach a certain displacement of the beam in a quadrupole. In other measurements the beam was supposed to go through the center of the quadrupole with a certain angle but no displacement. There is also the possibility to create a bump which combines these two applications. The principle how these bumps are created is the same.

Closed Orbit Bump Using 2 Correctors (π-bump)

The most simple closed orbit bump can be produced by two corrector magnets which have a betatron phase advance of $\psi = \pi$ according to Eq. 1.20. Consider the beam is moving on the ideal orbit (no imperfections). If a correction dipole gives the beam a kick of the angle κ_1 the beam will not be centered in the following magnets. At the place where the phase advance with respect to the correction magnet is π, the beam will have an angle of $-\kappa_1$ with respect to the ideal orbit. With another correction magnet at this place with the strength $\kappa_2 = \kappa_1$, the beam is deflected back to the ideal orbit. Outside the two magnets the beam moves on the ideal orbit. A schematic example of this type of closed orbit bump is shown in Fig. C.1.

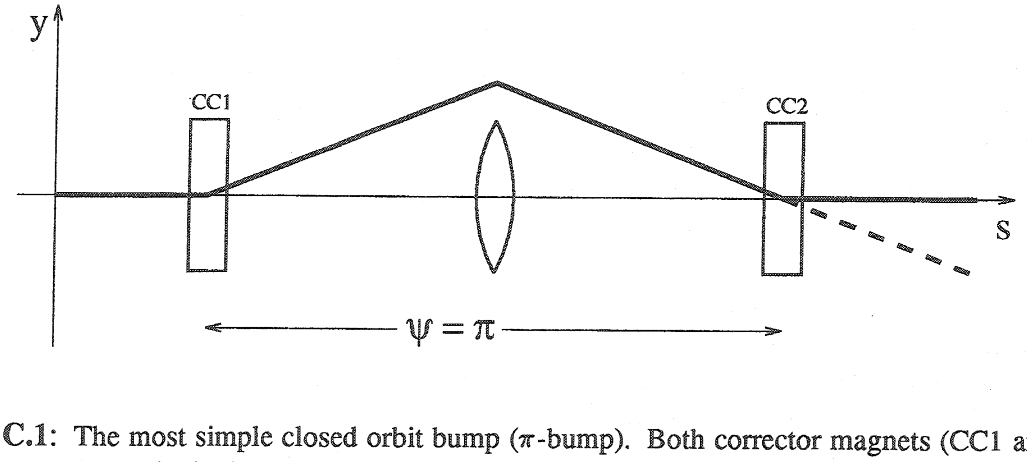

Figure C.1: The most simple closed orbit bump (π-bump). Both corrector magnets (CC1 and CC2) have the same strength. A phase advance of π between the two magnets is needed.

Closed Orbit Bump Using 3 Correctors

However one does not always have two correctors with a difference in phase advance of π. Therefore the use of at least three correction magnets is required. The first magnet works as in the previous example. The task of the second magnet is to give the beam a kick such that it only has an angle but no displacement in the third magnet which closes the bump. This is shown in Fig. C.2.

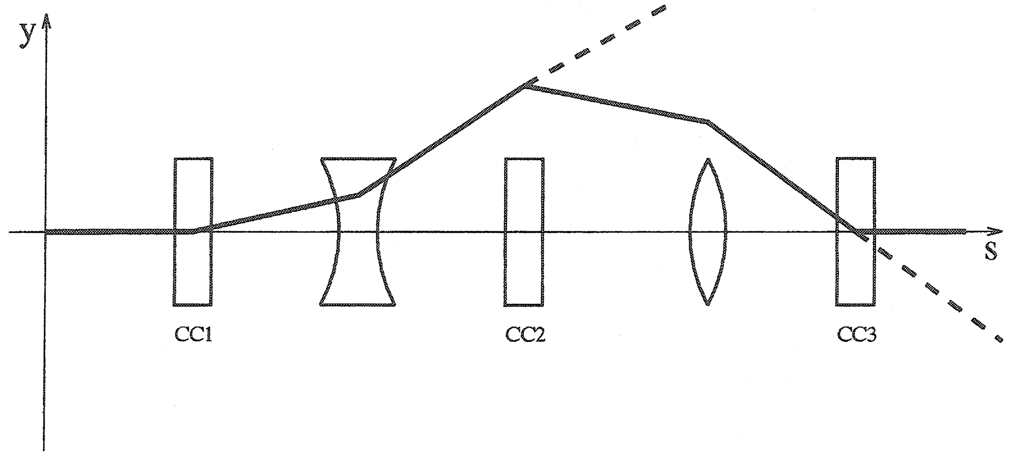

Figure C.2: A closed orbit bump using three correction magnets. Typically there are more quadrupoles between the correctors.

The strength of the kicks depend on the values of β at the corresponding points and on the phase advance between the magnets. A detailed description of how to calculate the kicks can be found in [Wil92].

Closed Orbit Bump Using 4 Correctors

To reach a certain displacement and a certain angle at a point P somewhere in the ring it is necessary to use four correction magnets. The only condition is that one needs two correction magnets on each side of the point where one wants to change the angle and/or the position of the beam. Those pairs of correctors can have any phase advance except multiples of π.

The first two correction magnets are used to bring the beam to the desired point with the desired angle. The third and the fourth magnet are used to bring the beam back to the ideal orbit. This is shown in Fig. C.3

The strengths of the kicks depend on the β-function and the phase advance ψ at the correction magnets and the point P and also on the value of α at P. They also depend on the desired angle and displacement. The equations for the strengths can be derived from the transfer matrices (see Chapter 1.5). Only the results are given here. κ_1 is the strength of the first corrector (CC1) and so forth. The subscripts denote which magnet (or the point P) is meant. The equations are taken from [Wil92]:

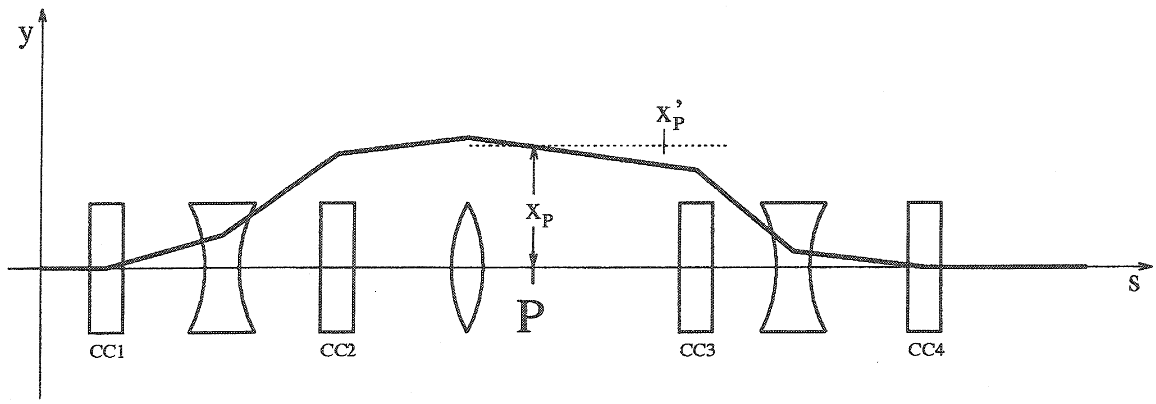

Figure C.3: A closed orbit bump using four correctors. The plot is very schematic. In LEP for example there are only correctors near every second quadrupole in the straight section.

$$\kappa_1 = \frac{1}{\sqrt{\beta_1\beta_P}}\frac{\cos(\psi_P-\psi_2)-\alpha_P\sin(\psi_P-\psi_2)}{\sin(\psi_2-\psi_1)}x_P - \sqrt{\frac{\beta_P}{\beta_1}}\frac{\sin(\psi_P-\psi_2)}{\sin(\psi_2-\psi_1)}x'_P \tag{C.1}$$

$$\kappa_2 = -\frac{1}{\sqrt{\beta_2\beta_P}}\frac{\cos(\psi_P-\psi_1)-\alpha_P\sin(\psi_P-\psi_1)}{\sin(\psi_2-\psi_1)}x_P + \sqrt{\frac{\beta_P}{\beta_2}}\frac{\sin(\psi_P-\psi_1)}{\sin(\psi_2-\psi_1)}x'_P \tag{C.2}$$

$$\kappa_3 = -\frac{1}{\sqrt{\beta_3\beta_P}}\frac{\cos(\psi_4-\psi_P)+\alpha_P\sin(\psi_4-\psi_P)}{\sin(\psi_4-\psi_3)}x_P - \sqrt{\frac{\beta_P}{\beta_3}}\frac{\sin(\psi_4-\psi_P)}{\sin(\psi_4-\psi_3)}x'_P \tag{C.3}$$

$$\kappa_4 = \frac{1}{\sqrt{\beta_4\beta_P}}\frac{\cos(\psi_3-\psi_P)+\alpha_P\sin(\psi_3-\psi_P)}{\sin(\psi_4-\psi_3)}x_P + \sqrt{\frac{\beta_P}{\beta_4}}\frac{\sin(\psi_3-\psi_P)}{\sin(\psi_4-\psi_3)}x'_P \tag{C.4}$$

Figure C.4 shows an example of a closed orbit bump that was used in our measurements. The strengths of the correction magnets were set in a way to displace the beam in the center of QS5.R8 by 1 mm without giving it an angle.

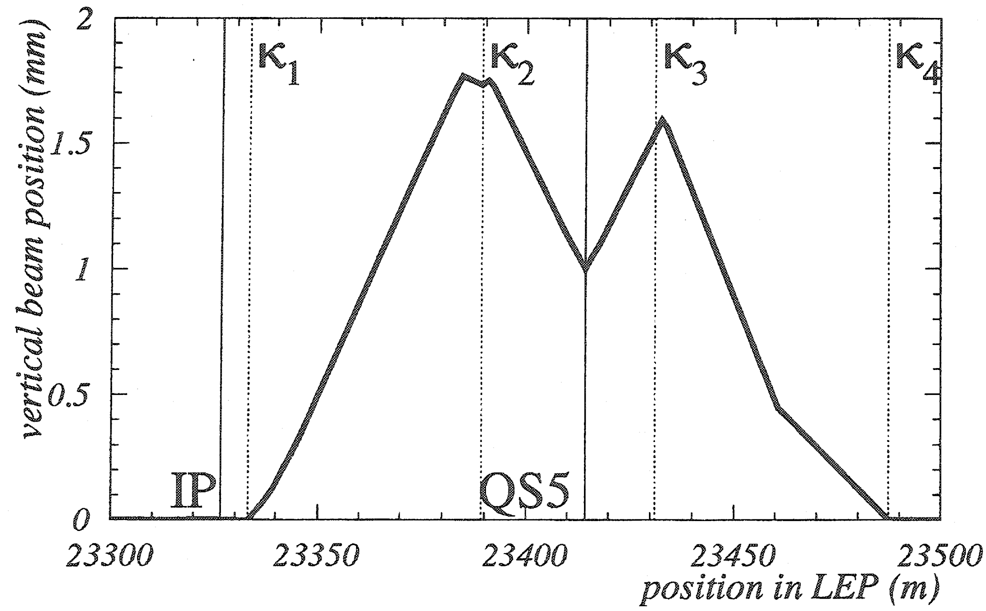

Figure C.4: Orbit between QS2.L8 and QS8.R8 using a local bump to move the beam by 1 mm in the vertical plane in the QS5.R8. The correctors are at the places indicated by dotted lines. The solid lines mark the positions of the QS5.R8 and the interaction point (IP). The positions of the other quadrupoles are not marked. The QS5 is vertically defocusing.

Abbreviations

ADC	analog digital converter
BOM	beam orbit monitor system
DSP	digital signal processor
FFT	(discrete) Fast-Fourrier-Transform
IP	interaction point
I/H	Integrate/Hold
MD	machine development
QS	straight section quadrupole (see p. 18)
RMS	root mean square

Bibliography

[Ass94] R. Assmann: *Transversale Spin-Polarisation und ihre Anwendung bei LEP*, PhD thesis at the Ludwigs-Maximilians-Universität München, 1994. To be published.

[Cham95] I. Barnett et al. *Do we need k-modulation in the Arcs?*, in Proceedings of the Fifth Workshop on LEP Performance, CERN SL/95-08 (DI), 1995.

[Bor93] J. Borer: *BOM system hardware status*, in Proceedings of the Third Workshop on LEP Performance, CERN SL/93-19 (DI), 1993.

[Bov94] C. Bovet: *LEP Beam Instrumentation*, in Proceedings of the Fourth Workshop on LEP Performance, CERN SL/94-06 (DI), 1994.

[CESR83] D. Rice et al.: *Beam Diagnostic Instrumentation at CESR*, in IEEE Transactions on Nuclear Science, Vol. NS-30, 1983.

[CESR85] R. Littauer: *Some Diagnostic Techniques Using Button Pickup Electrodes*, in Report of Machine Workshop on the 6-GeV Synchrotron Radiation Source, March 28-30, 1985, U.S. Department of Energy, Office of Basic Energy Sciences, Washington, D.C. 20545 and National Bureau of Standards, Gaithersburg, Maryland.

[Cocq91] D. Cocq: *Calibration du seuil des detecteurs du systeme BOM WB*, 1991, internal note, not published.

[Col94] P. Collier: *The Effect of Vertical Orbit on Luminosity via Dispersion and Coupling*, in Proceedings of the Fourth Workshop on LEP Performance, CERN SL/94-06 (DI), 1994.

[ECAL] L. Arnaudon et al.: *Accurate Determination of the LEP Beam Energy by Resonant Depolarization*, CERN SL/94-71 (BI), 1994.

[FFT] A detailed description of the algorithm can be found in W.H. Press et al.: *Numerical Recipes*, Cambridge University Press, 1989.

[HERA94] R. Brinkmann and M. Böge: *Beam-Based Alignment and Polarization Optimization in the HERA Electron Ring*, in Proceedings of the European Particle Accelerator Conference (EPAC), London, 1994.

[HSch94] MD done together with H. Schmickler; results not published yet.

[JRPS92] J. Rossbach & P. Schmüser: *Basic Course on Accelerator Optics*, in CERN Accelerator School: Proceedings of the Fifth General Accelerator Physics Course (1992), CERN, 94-01, 1994.

[LEP84] *LEP Design Report*, CERN-LEP/84-01, Vol. I and II, 1984.

[L3Col] The L3 Collaboration: *Results from the L3 Experiment at LEP*, CERN-PPE/93-31, 1993

[MAX94] P. Röjsel: *A Beam Position Measurement System Using Quadrupole Magnets Magnetic Centra as the Position Reference*, in Nuclear Instruments and Methods in Physics Research A 343, 1994.

[Mor] G. Morpurgo provided us with a copy of the software that calculates the beam position from the raw data.

[Par94] Physical Review D *Particles and Fields, Part I, Review of Particle Properties*, published by The American Physical Society, 1994.

[RSch93] R. Schmidt: *Misalignments from k-Modulation*, in Proceedings of the Third Workshop on LEP Performance, CERN SL/93-19 (DI), 1993.

[SLC91] Y. Chao et al.: *Alignment of the SLC Final Focus System Using Beam Orbits*, SLAC-PUB-5617 (1991), presented at the IEEE Particle Accelerator Conference, San Francisco, CA, 1991.

[Vis94] G. Vismara: *The New Front-End Narrow-Band Electronics for the LEP Beam Orbit Measurement System*, CERN SL/94-30 (BI), 1994.

[Vos] L. Vos and his group have installed the two couplers and kindly share the signals with us. It is descried in L. Vos: *Ground Motion in LEP and LHC*, SL 94-69 BI,1994.

[Wie93] H. Wiedemann: *Particle Accelerator Physics*, Springer, 1993.

[Wil92] K. Wille: *Physik der Teilchenbeschleuniger und Synchrotronstrahlungsquellen*, Teubner, 1992.

Acknowledgments

I would like to thank Mr. Priv. Doz. Dr. Manfred Tonutti for his initiative and for introducing me to the group at CERN which made this diploma work possible.

I owe Mr. Rüdiger Schmidt and his team a debt of gratitude for taking me in his group and giving me this interesting subject to work on. Also of course for constant support and interest.

I want thank Mr. Bernd Dehning for the help in the practical work especially whenever the electronics was concerned and for introducing me to the LEP operators and EICs.

I would like to thank Mr. Jörg Wenninger for helpful ideas and discussions and for the help with debugging my first FORTRAN-programs.

Many thanks to Mr. Frank Tecker for discussions and help with the measurements and for the nice picture of half a straight section (Fig. 2.2) and some of the histograms.

I would also like to acknowledge the help of Mr. Claude Bovet for his support and his secretary Mrs. Christa Parthe for dealing with the CERN bureaucracy.

I have to thank everybody working on the BOM especially Mr. Jean Borer and Mr. Giulio Morpurgo for supplying us with all the information they could give us and for kindly answering all my questions.

Many thanks to all the operators and EICs in the control room for allowing us to measure during physics-time. Special thanks Mr. Michael Jonker for help with the TG3-timing and to Mr. Hermann Schmickler for sharing his MD-time with us.

I want to thank Mr. Lucien Vos and his team for allowing us to use the signals from the couplers and supplying us with the information we needed.

I would like to thank the people in the magnet- and the power-converter-group for discussion and help, especially when the problems with the back-leg windings occured.

Thanks to Mr. Pedro Castro for the nice picture of a quadrupole (Fig.1.8).

I want to express my gratitude to numerous people from the SL division for support, help and discussion.

Höchster Dank gebührt meinen Eltern, die mir durch ihre Unterstützung mein Studium ermöglicht haben.